

Oscillatory motions of multiple spikes in three-component reaction-diffusion systems

Shuangquan Xie

xieshuangquan2013@gmail.com

Hunan University

Wen Yang

Wuhan Institute of Physics and Mathematics

Jiaojiao Zhang

Wuhan Institute of Physics and Mathematics

Research Article

Keywords: Multiple Hopf bifurcations, Coexistence of multiple oscillatory moving spikes, Matched asymptotic methods, Reduction methods, Three-Component reaction-diffusion systems.

Posted Date: September 6th, 2023

DOI: <https://doi.org/10.21203/rs.3.rs-3320061/v1>

License:  This work is licensed under a Creative Commons Attribution 4.0 International License.

[Read Full License](#)

Additional Declarations: No competing interests reported.

Version of Record: A version of this preprint was published at Journal of Nonlinear Science on June 28th, 2024. See the published version at <https://doi.org/10.1007/s00332-024-10058-y>.

Oscillatory motions of multiple spikes in three-component reaction-diffusion systems

Shuangquan Xie^{*}, Wen Yang[†] and Jiaojiao Zhang^{‡§}

September 2, 2023

Abstract

For three specific singular perturbed three-component reaction-diffusion systems that admit N -spike solutions in one of the components on a finite domain, we present a detailed analysis for the dynamics of temporal oscillations in the spike positions. The onset of these oscillations is induced by N Hopf bifurcations with respect to the translation modes that are excited nearly simultaneously. To understand the dynamics of N spikes in the vicinity of Hopf bifurcations, we combine the center manifold reduction and the matched asymptotic method to derive a set of ordinary differential equations (ODEs) of dimension $2N$ describing the spikes' locations and velocities, which can be recognized as normal forms of multiple Hopf bifurcations. The reduced ODE system then is represented in the form of linear oscillators with weakly nonlinear damping. By applying the multiple-time method, the leading order of the oscillation amplitudes is further characterized by an N -dimensional ODE system of the Stuart-Landau type. Although the leading order dynamics of these three systems are different, they have the same form after a suitable transformation. On the basis of the reduced systems for the oscillation amplitudes, we prove that there are at most $\lfloor N/2 \rfloor + 1$ stable equilibria, corresponding to $\lfloor N/2 \rfloor + 1$ types of different oscillations. This resolves an open problem proposed by Xie et al. (Nonlinearity, **34** (2021), pp. 5708-5743) for a three-component Schnakenberg system and generalizes the results to two other classic systems. Numerical simulations are presented to verify the analytic results.

Keywords— Multiple Hopf bifurcations, Coexistence of multiple oscillatory moving spikes, Matched asymptotic methods, Reduction methods, Three-Component reaction-diffusion systems.

Mathematics Subject Classification: 37L10, 35K57, 35B25, 35B36

1 Introduction

Spatially localized patterns have been observed in diverse physical and chemical experiments (see the survey [1]). The modeling of these experiments often generates nonlinear reaction-diffusion (RD) systems that admit spatial inhomogeneous solutions localized in small regions. As prototyping models to produce well-localized solutions, several well-known two-component RD systems, such as the Gierer–Meinhardt model [2], the Gray–Scott model [3] and the Schnakenberg model [4] have been extensively studied. In the large diffusivity ratio limit, these systems can exhibit multiple-spike solutions in the component with a slow diffusion rate. Such spiky patterns have been shown to exhibit various types of instabilities and dynamic behaviours such as spike splitting, temporal oscillations in the spike heights, spike annihilation, and slowly moving spike, see [5–11] and the book [12] for the Gierer–Meinhardt system, [13–18] for the Gray–Scott system, and [17, 19, 20] for the Schnakenberg system.

An intriguing phenomenon is the emergence of oscillatory patterns due to the Hopf bifurcation (HB). Typically, increasing the reaction ratio constant of the inhibitor or substrate can lead to a destabilization of the stationary spike solution through the HB. For the classic activator–inhibitor Gierer–Meinhardt model, the HB is subcritical and generates unstable time-periodic patterns with spikes oscillating in their heights [9, 10, 21, 22]. For the activator–substrate systems such as the Gray–Scott model and the Schnakenberg model, the HB for temporal

^{*}School of Mathematics, Hunan University, Changsha 410082, P. R. China. (xieshuangquan2013@gmail.com)

[†]Wuhan Institute of Physics and Mathematics, Innovation Academy for Precision Measurement Science and Technology, Chinese Academy of Sciences, Wuhan 430071, P. R. China. (math.yangwen@gmail.com)

[‡]University of Chinese Academy of Sciences, Beijing 100049, P. R. China.

[§]Wuhan Institute of Physics and Mathematics, Innovation Academy for Precision Measurement Science and Technology, Chinese Academy of Sciences, Wuhan 430071, P. R. China. (zhangjiaojiao@apm.ac.cn)

41 spike height oscillations occurs first and is subcritical at a low feeding rate [17, 21]. At a high feeding rate, the
 42 HB for temporal spike position oscillations occurs first and is supercritical [15, 23–25]. It is worth noting that
 43 the oscillation in the spike position requires both components in the system to be strongly coupled near the
 44 spike centers, namely, both the activator and the substrate are localized. One may ask whether it is possible to
 45 find stable oscillatory spikes in the positions with the substrate (inhibitor) weakly coupled with the activator.
 46 As far as the authors are aware, this appears to be unrealistic for two-component systems. On the other hand,
 47 theoretical results obtained for a class of three-component reaction-diffusion equations in [26] suggest that it is
 48 always feasible to find parameters that lead to the propagation of any stationary structure that can be found
 49 in the corresponding two-component system. This motivates us to consider three-component extensions of some
 50 classic two-component models. Recently, a three-component extension of the Schnakenberg model was analyzed
 51 in [27], exhibiting new, previously unobserved behaviour: numerical simulations reveal the coexistence of both
 52 in-phase and out-of-phase oscillations in the spike positions for a two-spike solution. An open problem proposed
 53 there is: *How many stable small-amplitude oscillatory moving patterns can we find for an N -spike solution when*
 54 *N translation modes are excited?* One goal of this paper is to address this problem.

55 In this paper, we consider three-component extensions of three singularly perturbed two-component systems

$$\begin{cases} u_t = \varepsilon^2 u_{xx} + f(u, v) - \kappa w, \\ 0 = Dv_{xx} + g(u, v), \\ \tau w_t = u - w, \\ \text{Neumann boundary conditions at } x = \pm 1. \end{cases} \quad x \in (-1, 1), \quad t \geq 0. \quad (1.1)$$

56 in the limit

$$\varepsilon \ll 1. \quad (1.2)$$

57 The first system is the Gierer-Meinhardt model with reaction terms as

$$f(u, v) = -(1 - \kappa)u + u^2/v, \quad g(u, v) = -v + \varepsilon^{-1}u^2. \quad (1.3)$$

58 The second system is the nondimensional Gray-Scott model at a low feeding rate with

$$f(u, v) = -(1 - \kappa)u + Au^2v, \quad g(u, v) = 1 - v - \varepsilon^{-1}u^2v. \quad (1.4)$$

59 The third system is the nondimensional Schnakenberg model at a low feeding rate with

$$f(u, v) = -(1 - \kappa)u + u^2v, \quad g(u, v) = \frac{1}{2} - \varepsilon^{-1}u^2v. \quad (1.5)$$

60 These three RD systems degenerate to their corresponding standard two-component systems when $\tau = 0$, which
 61 have the following two properties when $\varepsilon \ll 1$:

- 62 • When D satisfies some explicit constraints, there exists a stable N -spike solution with equal height.
- 63 • For a stable N -spike solution, the first N leading eigenvalues are negative real and $\mathcal{O}(\varepsilon^2)$, whose associated
 64 eigenmodes are translation modes in the leading order.

65 See [7, 18, 19] for related results on each model. Setting $\tau > 0$ does not change the equilibrium state but has
 66 an impact on the stability. In [26], the authors have shown that the eigenvalues that determine the stability
 67 of an equilibrium state in the extended systems (1.1) for general f and g can be explicitly determined by the
 68 eigenvalues of their two-component counterparts, suggesting that we can obtain some analytic results if we know
 69 the solution explicitly. For the systems under consideration, the first N leading eigenvalues are negative real and
 70 of the order ε^2 , allowing us to find N thresholds located within a region of width $\mathcal{O}(\varepsilon^2)$. These thresholds are
 71 identical in the limit $\varepsilon \rightarrow 0$, and N pairs of complex-conjugated eigenvalues pass through the imaginary axis as
 72 τ exceeds the critical value τ_c , which then excite the corresponding translation modes and initiate the multiple
 73 types of oscillations in the spike positions. We aim to understand the stable small-amplitude oscillatory patterns
 74 we can finally observe.

75 Fig. 1 illustrates the aforementioned phenomenon in the Schnakenberg model. For five spikes, there are five
 76 eigenvalues that cross the imaginary axis for τ slightly exceeding $\frac{1}{\kappa}$, which causes the spike center to oscillate
 77 periodically. The long-time dynamics settle into one of three possible stable oscillatory patterns, corresponding to
 78 the three stable equilibria in the amplitude equations. Which pattern is chosen depends on the initial conditions.
 79 For six spikes, there are six eigenvalues that cross the imaginary axis for values of τ well beyond $1/\kappa$. The
 80 long-time dynamics settle into one of four possible oscillatory stable patterns, corresponding to the four stable
 81 equilibria in the amplitude equations. Four types of oscillations coexist for the same parameter values, and the
 82 pattern selection mechanism depends only on the initial conditions.

83 With the goal to delineate the manifestation of periodically moving patterns, we perform a detailed study of
 84 temporal oscillations in the spike positions near Hopf bifurcations for N -spike solutions in three singular perturbed
 85 RD systems. In particular, we demonstrate that N Hopf modes become unstable when τ passes $\frac{1}{\kappa}$ in the limit

86 $\varepsilon \rightarrow 0$, leading to multiple types of oscillations at the onset of instability, which then saturate into a particular
 87 stable periodic orbit. Next, we perform a multiple-scale perturbation expansion in the vicinity of the bifurcation
 88 point and derive a set of ODE equations, explicitly describing the dynamics of multiple spikes. Finally, based
 89 on the reduced description, we prove that the leading order oscillations settle into one of the $\lfloor N/2 \rfloor + 1$ possible
 90 stable states.

91 The contribution of this paper is two-fold. First, we extend the results in [27] to another two classic RD
 92 systems, showing that the coexistence of multiple oscillation patterns is a universal phenomena. Second, we
 93 resolve the open problem raised in [27], giving a complete classification of the stable oscillation pattern slightly
 94 beyond multiple Hopf bifurcations.

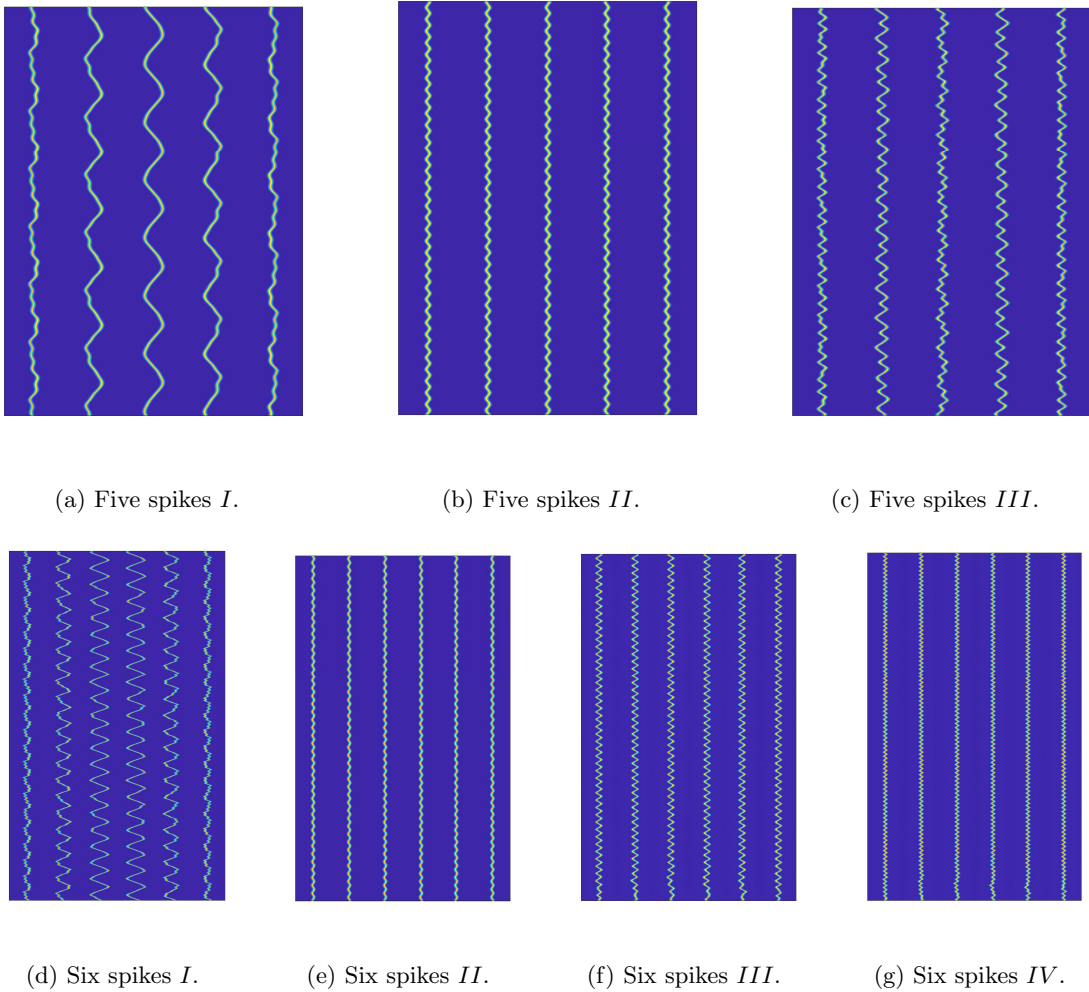


Figure 1: Space-time plots of the activator distribution u for different initial N -spike configurations obtained from numerically solving the system (1.1) using FlexPDE7 [28] with Schnakenberg type of nonlinearities in Eq. (1.5). The horizontal axis is space, and the vertical axis is time. The parameters are $\varepsilon = 0.005$, $\kappa = 0.8$, $D = \frac{1}{24N^3}$ for $N = 5, 6$. (a-c) three different final states of oscillatory five spikes at $\tau = 1.01/\kappa$. The only difference between them is the initial perturbation we select. (d-g) four different final states of oscillatory five spikes at $\tau = 1.015/\kappa$. The only difference between them is the initial perturbation we select.

95 The outline of this paper is as follows. In §2, we derive the relation between the eigenvalues of three-
 96 component systems and their associated two-component systems. We show that an N -spike solution undergoes
 97 a transition from a stationary state to an oscillatory state as the parameter τ is increased past some threshold
 98 τ_c ; this instability is triggered via a Hopf bifurcation of drift type. Moreover, N small eigenvalues (controlling
 99 the motion of N spikes) undergo Hopf bifurcations nearly simultaneously. Consequently, a complex interaction
 100 between the different modes can occur, leading to the coexistence of multiple possible oscillating patterns. A key

open problem then is determining whether these time-periodic solutions bifurcating from the N -spike stationary solution are stable.

In §3, we formally derive a reduced description of spike positions and velocities to unfold the dynamics near the bifurcation point for the Gierer-Meinhardt model, which is essentially the Hopf normal form. In general, this can be done by following the weakly nonlinear analysis developed in [22] or similar approaches used in [29]. However, the leading eigenmode in these references is associated with an $\mathcal{O}(1)$ eigenvalue, in contrast with $\mathcal{O}(\varepsilon^2)$ eigenvalue in this article. Moreover, only one Hopf mode is assumed to be excited in [22] and [29], while we study the scenario when multiple Hopf modes are excited. These differences make our problem more delicate and require intricate analysis in a hierarchy of problems in each order of ε . We will use a combination of the matched asymptotic methods and the center manifold reduction to reduce the PDE system to a set of ODE systems up to $\mathcal{O}(\varepsilon^2)$. We then apply the multiple-scale method to obtain a leading order approximation of the solution to the reduced system, revealing that the spikes oscillations consist of different oscillating modes in the leading order of ε , whose amplitudes are subject to a system of ordinary differential equations that can be seen as the Landau equations. Each equilibrium point of the amplitude equations corresponds to an oscillatory state, the stability of which determines the final state we can observe numerically.

In §4, we classify the equilibria of the amplitude equations with respect to τ and rigorously prove that the Landau equations have at most 2^N non-negative equilibria, among which $\lfloor N/2 \rfloor + 1$ are stable, suggesting that at most $\lfloor N/2 \rfloor + 1$ stable small-amplitude oscillatory pattern can be observed in the leading order. Finally, in §5 we summarize our results and highlight some open problems for future research.

2 Hopf Bifurcations

In this section, we investigate the bifurcations induced by increasing the reaction ratio τ for general three-component systems (1.1). The analysis for the extended Schnakenberg model has been carried out in [27]. Here we sketch the analysis for a general system. We consider the dynamics linearized around the stationary solution (u_s, v_s, u_s) and compare it with the dynamics in the special case $\tau = 0$.

We define the linear operator \mathcal{L}_0 as follows:

$$\mathcal{L}_0 := \begin{pmatrix} \varepsilon^2 \Delta + f_u(u_s, v_s) - \kappa & f_v(u_s, v_s) \\ g_u(u_s, v_s) & D\Delta + g_v(u_s, v_s) \end{pmatrix}. \quad (2.1)$$

For a perturbation $[\phi_\tau, \psi_\tau, \eta_\tau] \ll 1$ to the steady state $[u_s, v_s, u_s]$, we obtain the following eigenvalue problem for $\tau = 0$:

$$\gamma \phi_0 = \varepsilon^2 \Delta \phi_0 + f_u(u_s, v_s) \phi_0 + f_v(u_s, v_s) \psi_0 - \kappa \eta_0, \quad (2.2a)$$

$$0 = D\Delta \psi_0 + g_u(u_s, v_s) \phi_0 + g_v(u_s, v_s) \psi_0, \quad (2.2b)$$

$$0 = \phi_0 - \eta_0; \quad (2.2c)$$

and for $\tau \neq 0$:

$$\lambda \phi_\tau = \varepsilon^2 \Delta \phi_\tau + f_u(u_s, v_s) \phi_\tau + f_v(u_s, v_s) \psi_\tau - \kappa \eta_\tau, \quad (2.3a)$$

$$0 = D\Delta \psi_\tau + g_u(u_s, v_s) \phi_\tau + g_v(u_s, v_s) \psi_\tau, \quad (2.3b)$$

$$\tau \lambda \eta_\tau = \phi_\tau - \eta_\tau, \quad (2.3c)$$

where we denote the eigenvalues of the three-component system at $\tau = 0$ as γ and the eigenvalues at $\tau \neq 0$ as λ . The system Eq. (2.2) can be rewritten as

$$\gamma \begin{pmatrix} \phi_0 \\ \psi_0 \end{pmatrix} = \mathcal{L}_0 \begin{pmatrix} \phi_0 \\ \psi_0 \end{pmatrix}, \quad (2.4)$$

Note that the third row of system Eq. (2.3) is a linear algebraic equation. We solve η_τ w.r.t ϕ_τ to obtain

$$\eta_\tau = \frac{1}{1 + \tau \lambda} \phi_\tau. \quad (2.5)$$

Using this to remove η_τ in other two rows, we obtain

$$\lambda \left(1 - \frac{\kappa \tau}{1 + \tau \lambda} \right) \begin{pmatrix} \phi_\tau \\ \psi_\tau \end{pmatrix} = \mathcal{L}_0 \begin{pmatrix} \phi_\tau \\ \psi_\tau \end{pmatrix}. \quad (2.6)$$

Comparing Eq. (2.4) and Eq. (2.6), we compute λ and $[\phi_\tau, \psi_\tau, \eta_\tau]$ based on γ and $[\phi_0, \psi_0, \eta_0]$ as follows:

$$\lambda = \frac{\tau(\kappa + \gamma) - 1}{2\tau} \pm \sqrt{\frac{\gamma}{\tau} + \left(\frac{\tau(\kappa + \gamma) - 1}{2\tau} \right)^2}, \quad (2.7a)$$

$$[\phi_\tau, \psi_\tau, \eta_\tau] = [\phi_0, \psi_0, \frac{1}{1 + \tau\lambda}\eta_0]. \quad (2.7b)$$

Eq. (2.7) implies that the eigenvalue and eigenvector at $\tau \neq 0$ can be directly obtained from those at $\tau = 0$. When τ is increased, the bifurcations detected are ranked according to the value of the related γ . Thus, if an N -spike solution is stable for $\tau = 0$, this solution will stay stable until τ is increased up to $\frac{1}{\kappa + \gamma_{\max}}$.

We are interested in the stability of an N -spike solution and the dynamics of N spikes in the vicinity of the bifurcation. Denote the u component of an N -spike quasi-equilibrium solution as

$$u_s \sim \sum_{k=1}^N u_c \left(\frac{x - x_k}{\varepsilon} \right), \quad (2.8)$$

where x_k is the equilibrium position, $\{x_k = -1 + \frac{2k-1}{N}, k = 1, \dots, N\}$. For the systems we consider in this paper, the first N leading eigenvalues $\{\gamma_k, k = 1, \dots, N\}$ are negative real and of the order ε^2 (see the computations in [7, 18, 19]). Hence, increasing the bifurcation parameter τ to pass $\tau_k := \frac{1}{\kappa + \gamma_k}$ pushes the k -th eigenvalue to cross the imaginary axis with pure imaginary numbers. Since the eigenvector corresponding to γ_k is a translation mode that can be written as a linear combination of $\{u'_c(\frac{x-x_k}{\varepsilon}), k = 1, \dots, N\}$, N translation modes are destabilized when $\tau > \tau_N$, leading to complex motions in the spike positions. In the limit $\varepsilon \ll 1$, we have $\tau_k \sim \frac{1}{\kappa}$ for $k = 1, \dots, N$, then N Hopf modes become excited almost simultaneously when τ is above $\tau_c := \frac{1}{\kappa}$.

Now we give a rough description of the dynamics near the bifurcation point. We denote the ϕ component of corresponding first N eigenvectors as

$$\phi_{0,k} \sim \sum_{j=1}^N Q_{j,k} u'_c \left(\frac{x - x_j}{\varepsilon} \right), \quad k = 1, \dots, N, \quad (2.9)$$

where $Q_{j,k}$ are constants determining the moving direction of j -th spike under the influence of k -th mode $\phi_{0,k}$. We define Q as the matrix with $Q_{j,k}$ as its entries,

$$Q := \{Q_{j,k}\} = (\mathbf{q}_1, \dots, \mathbf{q}_N). \quad (2.10)$$

For the Schnakenberg model, the Gierer-Meinhardt model and the Gray-Scot model, they have the same Q (see [7, 18, 19]) that can be computed as

$$\mathbf{q}_N = \sqrt{\frac{1}{N}} [1, -1, 1, \dots, (-1)^{N+1}]^\top, \quad (2.11a)$$

$$\mathbf{q}_k = [Q_{1,k}, \dots, Q_{N,k}]^\top, \quad k = 1, \dots, N-1, \quad (2.11b)$$

$$Q_{j,k} = \sqrt{\frac{2}{N}} \sin\left(\frac{\pi k}{N}(j - \frac{1}{2})\right). \quad (2.11c)$$

Here $[\cdot]^\top$ denotes the transpose. If we increase the control parameter τ slightly beyond τ_c as $\tau = \tau_c + \varepsilon^2 \hat{\tau}$, these N translation modes dominate the dynamics. Then, the dynamics can be approximated by

$$u \sim \sum_{k=1}^N u_c \left(\frac{x - x_k}{\varepsilon} \right) + \sum_{k=1}^N (A_k e^{\lambda_k t} \phi_{0,k} + \text{c.c.}), \quad (2.12)$$

where A_k are constant oscillation amplitudes and c.c. is referred to as the complex conjugate. We rewrite λ_k as

$$\lambda_k = \varepsilon^2 \mu_k + \mathcal{O}(\varepsilon^3) + i(\varepsilon \omega_k + \mathcal{O}(\varepsilon^2)), \quad (2.13)$$

then the corresponding factor $e^{\lambda_k t}$ in Eq. (2.12) can be decomposed into the oscillatory factor $e^{i\varepsilon \omega_k t}$ and the growth factor $e^{\varepsilon^2 \mu_k t}$. Including the growth factor into the complex amplitude A_k yields,

$$u \sim \sum_{k=1}^N u_c \left(\frac{x - x_k}{\varepsilon} \right) + \sum_{k=1}^N (A_k(\varepsilon^2 t) e^{i\varepsilon \omega_k t} \phi_{0,k} + \text{c.c.}) \sim \sum_{k=1}^N u_c \left(\frac{x - x_k - \varepsilon p_k}{\varepsilon} \right), \quad (2.14)$$

where $p_k = \sum_{j=1}^N Q_{j,k} B_j(\varepsilon^2 t) \cos(\varepsilon \omega_j t + \theta_j(\varepsilon^2 t))$ and B_j is the amplitude of the oscillation with the frequency ω_k whose slow evolution requires a high order analysis. The ODE system describing the dynamics of B_j for the Schnakenberg model has been derived in [27], where the method of matched asymptotic analysis and the method of multiple scales are utilized. Our goal in the next section is to write down the ordinary differential equation of the amplitude B_j for the other two systems.

3 Slow dynamics close to the Hopf bifurcation

In this section, we investigate the dynamics in the vicinity of N -fold Hopf bifurcations by projecting the dynamics into the space expanded by N excited translation modes. As the eigenvalues have a different scaling in real and imaginary part when $\tau = \frac{1}{\kappa} + \hat{\tau}\varepsilon^2$, the analysis involves different orders of ε . We will derive the dynamics by a combination of the matched asymptotic methods and the center manifold reduction. The derivation has been done for the Schnakenberg model in [27], we take the same strategy to derive the reduced dynamics for the Gierer-Meinhardt model. As to the Gray-Scott model, we omit the derivation and only present the results.

3.1 Reduced ODE system for the Gierer-Meinhardt model

We consider the extended Gierer-Meinhardt system:

$$\begin{cases} u_t = \varepsilon^2 u_{xx} - (1 - \kappa)u + u^2/v - \kappa w, \\ 0 = Dv_{xx} - v + u^2/\varepsilon, \\ \tau w_t = u - w, \\ \text{Neumann boundary conditions at } x = \pm 1. \end{cases} \quad (3.1)$$

For a initial condition with N spikes located at positions close to their equilibrium positions, the spikes will start to oscillate with a small amplitude when τ slightly exceeds $\frac{1}{\kappa}$; thus we assume the k -th spike to be located at $\hat{x}_k = x_k + \varepsilon p_k$ according to Eq. (2.14). Then, we calculate the solution in the inner region near the k -th spike where $|x - \hat{x}_k| \sim \mathcal{O}(\varepsilon)$, and in the outer region away from the k -th spike where $|x - \hat{x}_k| \sim \mathcal{O}(1)$. The equations for the position of each spike are determined by matching the outer and inner solutions.

Inner region: Near the k -th spike, we introduce variable $y = \frac{x - x_k - \varepsilon p_k(t)}{\varepsilon}$, and rewrite u, v and w as

$$u(x, t) = U(y, t), \quad v(x, t) = V(y, t), \quad w(x, t) = W(y, t). \quad (3.2)$$

Then, the system (3.1) becomes

$$-U_y \dot{p}_k + \frac{\partial U}{\partial t} = U_{yy} - (1 - \kappa)U + U^2/V - \kappa W, \quad (3.3a)$$

$$0 = DV_{yy} - \varepsilon^2 V + \varepsilon U^2, \quad (3.3b)$$

$$\left(\frac{1}{\kappa} + \varepsilon^2 \hat{\tau}\right) \left(-W_y \dot{p}_k + \frac{\partial W}{\partial t}\right) = U - W. \quad (3.3c)$$

The far-field conditions as $|y| \rightarrow \infty$ are that U and W tend to zero exponentially, whereas the conditions for V contain some constants that must be determined by matching with the outer solution.

To facilitate the analysis, we introduce slow time scales

$$T_1 = \varepsilon t, \quad T_2 = \varepsilon^2 t, \dots,$$

so that

$$\dot{p}_k = \varepsilon \frac{\partial p_k}{\partial T_1} + \varepsilon^2 \frac{\partial p_k}{\partial T_2} + \dots, \quad (3.4)$$

and use the following expansion according to Eq. (2.7b)

$$\begin{bmatrix} U \\ V \\ W \end{bmatrix} = \begin{bmatrix} U_0 \\ V_0 \\ W_0 \end{bmatrix} + \varepsilon \left(\begin{bmatrix} U_1 \\ V_1 \\ W_1 \end{bmatrix} + \alpha_k \begin{bmatrix} 0 \\ 0 \\ U_{0y} \end{bmatrix} \right) + \varepsilon^2 \begin{bmatrix} U_2 \\ V_2 \\ W_2 \end{bmatrix} + \varepsilon^3 \begin{bmatrix} U_3 \\ V_3 \\ W_3 \end{bmatrix} + h.o.t., \quad (3.5)$$

with $[U_0, V_0, W_0]$ being the spike profile and $[U_k, V_k, W_k]$ being orthogonal to $[U_{0y}, V_{0y}, U_{0y}]$ and $[0, 0, U_{0y}]$ for $k \geq 1$. Note that $[U_{0y}, V_{0y}, U_{0y}]$ has been implicitly included into $[U_0, V_0, U_0]$ in the way of Eq. (2.14). Substituting Eq. (3.5) and Eq. (3.4) into Eq. (3.3) and collecting different terms in order of ε , we obtain a hierarchy of equations.

In the leading order, we obtain

$$0 = U_{0yy} - (1 - \kappa)U_0 + U_0^2/V_0 - \kappa W_0, \quad (3.6a)$$

$$0 = DV_{0yy}, \quad (3.6b)$$

$$0 = U_0 - W_0. \quad (3.6c)$$

The conditions needed to match to the outer solution are that V_0 is bounded and $U_0, W_0 \rightarrow 0$ as $|y| \rightarrow \infty$. Thus, the solution to Eq. (3.6) is

$$U_0 = c_{k,0}\rho(y), \quad V_0 = c_{k,0}, \quad W_0 = c_{k,0}\rho(y), \quad (3.7)$$

182 where $c_{k,0}$ are constants we will determine by matching and $\rho(y) = \frac{3}{2}\text{sech}^2(\frac{y}{2})$ satisfying

$$\rho'' - \rho + \rho^2 = 0; \quad \rho \rightarrow 0 \text{ as } |y| \rightarrow \infty; \quad \rho'(0) = 0. \quad (3.8)$$

183 Since V_0 is a constant, the orthogonal conditions are simplified to be

$$\langle U_k, U_{0y} \rangle = 0, \quad \langle W_k, U_{0y} \rangle = 0, \text{ for } k \geq 1 \quad (3.9)$$

184 where $\langle f, g \rangle$ denotes the inner product of two functions over \mathbb{R} ,

$$\langle f, g \rangle := \int_{-\infty}^{\infty} f(y)g(y) dy. \quad (3.10)$$

In the order of ε , we obtain

$$-U_{0y} \frac{\partial p_k}{\partial T_1} - \mathcal{F}_1 = U_{1yy} - (1 - \kappa)U_1 + 2U_0U_1/V_0 - \kappa(W_1 + \alpha_k U_{0y}), \quad (3.11a)$$

$$0 = DV_{1yy} + U_0^2, \quad (3.11b)$$

$$-W_{0y} \frac{\partial p_k}{\partial T_1} = \kappa(U_1 - (W_1 + \alpha_k U_{0y})), \quad (3.11c)$$

185 where

$$\mathcal{F}_1 := -U_0^2 V_1 / V_0^2. \quad (3.12)$$

186 Since V_1 is independent of U_1 and W_1 , we solve Eq. (3.11b) for V_1 first to obtain

$$V_1 = c_{k,0}^2 g_1 + b_{k,1}y + c_{k,1}, \quad (3.13)$$

187 where $b_{k,1}$, $c_{k,1}$ are constants left to be determined and g_1 is an even function defined as

$$g_1 := -\frac{1}{D} \int_0^y \int_0^z \rho^2 d\hat{y} dz. \quad (3.14)$$

188 The far field behavior of V_1 is

$$V_1 \rightarrow (c_{k,0}^2 g_1'(\pm\infty) + b_{k,1})y + \left[c_{k,1} - \frac{c_{k,0}^2}{D} \int_0^{\pm\infty} \int_{\pm\infty}^y \rho^2 dz dy \right], \text{ as } y \rightarrow \pm\infty, \quad (3.15)$$

189 Since g_1' is odd, the constant $b_{k,1}$ can be determined by the far field behaviour of V_1' :

$$b_{k,1} = \frac{1}{2} (V_1'(+\infty) + V_1'(-\infty)). \quad (3.16)$$

190 Using Eq. (3.11c) to remove W_1 in Eq. (3.11a) yields

$$U_{1yy} - U_1 + 2\rho U_1 = -\mathcal{F}_1. \quad (3.17)$$

191 Since U_{0y} is the homogeneous solution of Eq. (3.17), the right hand side of Eq. (3.17) must be orthogonal to U_{0y} .

192 Taking the inner product between Eq. (3.17) and U_{0y} gives rise to the solvability condition of Eq. (3.17):

$$-\langle U_{0y}, \mathcal{F}_1 \rangle = 0, \quad (3.18)$$

193 Using the fact that U_{0y} is odd and V_1 can be decomposed as the addition of odd and even functions, we obtain

$$b_{k,1} \int_{-\infty}^{\infty} \rho^2 \rho' y dy = 0. \quad (3.19)$$

194 Thus, the solvability condition yields

$$b_{k,1} = 0. \quad (3.20)$$

195 Using Eq. (3.20), we solve Eq. (3.11a) for U_1 to obtain

$$U_1 = c_{k,1}\rho + c_{k,0}^2 f_1, \quad (3.21)$$

196 where f_1 is an even function satisfying

$$f_1'' - f_1 + 2\rho f_1 = \rho^2 g_1. \quad (3.22)$$

197 Taking the inner product between Eq. (3.11c) and U_{0y} and using the orthogonal condition Eq. (3.9) yield

$$\frac{\partial p_k}{\partial T_1} = \kappa \alpha_k. \quad (3.23)$$

198 Substituting Eq. (3.23) into Eq. (3.11c), we obtain

$$W_1 = U_1. \quad (3.24)$$

In the order of ε^2 , we obtain

$$-U_{0y} \frac{\partial p_k}{\partial T_2} - U_{1y} \frac{\partial p_k}{\partial T_1} + \frac{\partial U_1}{\partial T_1} - \mathcal{F}_2 = U_{2yy} - (1 - \kappa)U_2 + 2U_0U_2/V_0 - \kappa W_2, \quad (3.25a)$$

$$0 = DV_{2yy} - V_0 + 2U_0U_1, \quad (3.25b)$$

$$-W_{0y} \frac{\partial p_k}{\partial T_2} - (W_{1y} + \alpha_k U_{0yy}) \frac{\partial p_k}{\partial T_1} + U_{0y} \frac{\partial \alpha_k}{\partial T_1} + \frac{\partial W_1}{\partial T_1} = \kappa(U_2 - W_2), \quad (3.25c)$$

199 where

$$\mathcal{F}_2 := U_1^2/V_0 - 2U_0U_1V_1/V_0^2 - U_0^2V_2/V_0^2 + U_0^2V_1^2/V_0^3. \quad (3.26)$$

200 Solving Eq. (3.25b) for V_2 , we obtain

$$\begin{aligned} V_2 &= \frac{1}{D} \int_0^y \int_0^z (V_0 - 2U_0U_1) d\hat{y}dz + b_{k,2}y + c_{k,2} \\ &= \frac{1}{2D} c_{k,0}y^2 + b_{k,2}y + c_{k,2} + 2c_{k,0}c_{k,1}g_1 + 2c_{k,0}^3g_2, \end{aligned} \quad (3.27)$$

201 where $b_{k,2}$, $c_{k,2}$ are constants determined by matching with the outer region and g_2 is defined as

$$g_2 := -\frac{1}{D} \int_0^y \int_0^z \rho f_1 d\hat{y}dz. \quad (3.28)$$

202 Note that $b_{k,2}$ can be determined by the far field behavior of V_2' as follows:

$$b_{k,2} = \frac{1}{2} (V_2'(+\infty) + V_2'(-\infty)). \quad (3.29)$$

203 Using Eq. (3.25c) and Eq. (3.24) to remove W_2 in Eq. (3.25a) yields

$$U_{2yy} - U_2 + 2\rho U_2 = -\mathcal{F}_2 + U_{0yy} \frac{\partial p_k}{\partial T_1} \alpha_k - U_{0y} \frac{\partial \alpha_k}{\partial T_1}. \quad (3.30)$$

204 Taking the inner product between Eq. (3.30) and U_{0y} gives rise to

$$\frac{\partial \alpha_k}{\partial T_1} = -\frac{\langle \mathcal{F}_2, U_{0y} \rangle}{\langle U_{0y}, U_{0y} \rangle} + \frac{\langle U_{0yy}, U_{0y} \rangle}{\langle U_{0y}, U_{0y} \rangle} \frac{\partial p_k}{\partial T_1} \alpha_k. \quad (3.31)$$

205 Note that only the inner product between U_{0y} and the odd part of \mathcal{F}_2 is nonzero. We simplify Eq. (3.31) as

$$\frac{\partial \alpha_k}{\partial T_1} = \frac{b_{k,2} \int_{-\infty}^{\infty} \rho^2 \rho' y dy}{c_{k,0} \int_{-\infty}^{\infty} \rho'^2 dy}, \quad (3.32)$$

206 We rewrite U_2 as a summation of an even function and an odd function

$$U_2 = U_{2,e} + U_{2,o}, \quad (3.33)$$

207 where $U_{2,e}$ and $U_{2,o}$ satisfy:

$$U_{2,eyy} - U_{2,e} + 2\rho U_{2,e} = -U_1^2/V_0 + 2U_0U_1V_1/V_0^2 + U_0^2V_{2,e}/V_0^2 - U_0^2V_1^2/V_0^3 + U_{0yy} \frac{\partial p_k}{\partial T_1} \alpha_k, \quad (3.34)$$

208

$$U_{2,oyy} - U_{2,o} + 2\rho U_{2,o} = U_0^2V_{2,o}/V_0^2 - U_{0y} \frac{\partial \alpha_k}{\partial T_1}. \quad (3.35)$$

209 For latter use, we express $U_{2,e}$ and $U_{2,o}$ as

$$U_{2,e} = c_{k,1}c_{k,0}e_1 + c_{k,2}\rho + c_{k,0}e_2 + c_{k,0}^3e_3 + \frac{c_{k,0}\kappa\alpha_k^2}{2}y\rho', \quad (3.36)$$

210

$$U_{2,o} = b_{k,2}f_2, \quad (3.37)$$

211 where e_j , $j = 1, \dots, 3$, are even and f_2 is odd, satisfying

$$e_1'' - e_1 + 2\rho e_1 = 2\rho^2g_1, \quad (3.38a)$$

212

$$e_2'' - e_2 + 2\rho e_2 = \frac{1}{2D}\rho^2 y^2, \quad (3.38b)$$

213

$$e_3'' - e_3 + 2\rho e_3 = -f_1^2 + 2\rho g_1 f_1 + 2\rho^2 g_2 - \rho^2 g_1^2, \quad (3.38c)$$

214

$$f_2'' - f_2 + 2\rho f_2 = \rho^2 y - \frac{\rho' \int_{-\infty}^{\infty} \rho^2 \rho' y dy}{\int_{-\infty}^{\infty} \rho'^2 dy}. \quad (3.38d)$$

215 Taking the inner product between Eq. (3.25c) and U_{0y} and using the orthogonal condition Eq. (3.9) yield

$$\frac{\partial p_k}{\partial T_2} = \frac{\partial \alpha_k}{\partial T_1} - \frac{\langle W_{1y} + \alpha_k U_{0yy}, U_{0y} \rangle}{\langle U_{0y}, U_{0y} \rangle} \frac{\partial p_k}{\partial T_1}. \quad (3.39)$$

216 Note that

$$\langle W_{1y} + \alpha_k U_{0yy}, U_{0y} \rangle = \langle U_{1y} + \alpha_k U_{0yy}, U_{0y} \rangle = \langle U_{1y}, U_{0y} \rangle = c_{k,0} c_{k,1} \int_{-\infty}^{\infty} \rho'^2 dy + c_{k,0}^3 \int_{-\infty}^{\infty} f_{1y} \rho' dy. \quad (3.40)$$

217 Thus,

$$\frac{\partial p_k}{\partial T_2} = \frac{b_{k,2} \int_{-\infty}^{\infty} \rho^2 \rho' y dy}{c_{k,0} \int_{-\infty}^{\infty} \rho'^2 dy} - \frac{c_{k,1} \int_{-\infty}^{\infty} \rho'^2 dy + c_{k,0}^2 \int_{-\infty}^{\infty} f_{1y} \rho' dy}{c_{k,0} \int_{-\infty}^{\infty} \rho'^2 dy} \kappa \alpha_k. \quad (3.41)$$

218 Substituting Eq. (3.39) into Eq. (3.25c), we obtain

$$W_2 = U_2 + \frac{1}{\kappa} (W_{1y} + \alpha_k U_{0yy}) \frac{\partial p_k}{\partial T_1} - \frac{1}{\kappa} \frac{\langle W_{1y}, U_{0y} \rangle}{\langle U_{0y}, U_{0y} \rangle} \frac{\partial p_k}{\partial T_1} U_{0y}. \quad (3.42)$$

219 In the order of ε^3 , we obtain

$$-U_{0y} \frac{\partial p_k}{\partial T_3} - U_{1y} \frac{\partial p_k}{\partial T_2} + \frac{\partial U_1}{\partial T_2} + \frac{dU_2}{dT_1} - \mathcal{F}_3 = U_{3yy} - (1 - \kappa)U_3 + 2U_0 U_3 / V_0 - \kappa W_3, \quad (3.43a)$$

220

$$0 = DV_{3yy} - V_1 + 2U_0 U_2 + U_1^2, \quad (3.43b)$$

221

$$-\hat{\tau} \kappa \frac{\partial p_k}{\partial T_1} U_{0y} - W_{0y} \frac{\partial p_k}{\partial T_3} - (W_{1y} + \alpha_k U_{0yy}) \frac{\partial p_k}{\partial T_2} + U_{0y} \frac{\partial \alpha_k}{\partial T_2} + \frac{\partial W_1}{\partial T_2} + \frac{dW_2}{dT_1} = \kappa (U_3 - W_3). \quad (3.43c)$$

222 where

$$\mathcal{F}_3 := (2U_0^2 V_1 V_2 + 2U_1 U_2 V_0^2 + 2U_0 U_1 V_1^2 - 2U_0 U_1 V_0 V_2 - (U_1^2 + 2U_0 U_2) V_1 V_0 - U_0^2 V_3 V_0 - U_0^2 V_1^3 / V_0) / V_0^3. \quad (3.44)$$

223 Solving Eq. (3.43b), we obtain

$$V_3 = \frac{1}{D} \int_0^y \int_0^z (V_1 - 2U_0 U_2 - U_1^2) d\hat{y} dz + b_{k,3y} + c_{k,3}, \quad (3.45)$$

224 where $b_{k,3}$, $c_{k,3}$ are constants determined by matching with the outer region. We rewrite V_3 as the sum of an
225 even function $V_{3,e}$ and an odd function $V_{3,o}$:

$$V_3 = V_{3,e} + V_{3,o}. \quad (3.46)$$

226 Then,

$$V_{3,o} = b_{k,3y} + 2b_{k,2} c_{k,0} g_3. \quad (3.47)$$

227 where g_3 is an odd function defined as

$$g_3 := -\frac{1}{D} \int_0^y \int_0^z \rho f_2 d\hat{y} dz. \quad (3.48)$$

228 Note that $b_{k,3}$ can be determined by the far field behavior of V_3' as follow:

$$b_{k,3} = \frac{1}{2} (V_3'(+\infty) + V_3'(-\infty)) + \frac{2b_{k,2} c_{k,0}}{D} \int_0^\infty \rho f_2 dy. \quad (3.49)$$

229 Using Eq. (3.43c) to remove W_3 in Eq. (3.43a) yields

$$U_{3yy} - U_3 + 2\rho U_3 = \hat{\tau} \kappa \frac{\partial p_k}{\partial T_1} U_{0y} + \alpha_k U_{0yy} \frac{\partial p_k}{\partial T_2} - U_{0y} \frac{\partial \alpha_k}{\partial T_2} + \frac{d(U_2 - W_2)}{dT_1} - \mathcal{F}_3. \quad (3.50)$$

230 Taking the inner product between Eq. (3.50) and U_{0y} gives rise to

$$\frac{\partial \alpha_k}{\partial T_2} = \hat{\tau} \kappa \frac{\partial p_k}{\partial T_1} + \frac{\langle \frac{d(U_2 - W_2)}{dT_1}, U_{0y} \rangle}{\langle U_{0y}, U_{0y} \rangle} + \alpha_k \frac{\partial p_k}{\partial T_2} \frac{\langle U_{0y}, U_{0yy} \rangle}{\langle U_{0y}, U_{0y} \rangle} - \frac{\langle \mathcal{F}_3, U_{0y} \rangle}{\langle U_{0y}, U_{0y} \rangle}. \quad (3.51)$$

231 We now compute each of the terms on the right hand side of Eq. (3.51). Integrating by parts and using Eq. (3.9),
 232 Eq. (3.25c), Eq. (3.23), Eq. (3.24), we calculate

$$\begin{aligned} \left\langle \frac{d(U_2 - W_2)}{dT_1}, U_{0y} \right\rangle &= \frac{d}{dT_1} \langle U_2 - W_2, U_{0y} \rangle - \langle U_2 - W_2, -\frac{\partial p_k}{\partial T_1} U_{0yy} \rangle \\ &= 0 - \frac{1}{\kappa} \langle W_{1y} + \alpha_k U_{0yy}, U_{0yy} \rangle \left(\frac{\partial p_k}{\partial T_1} \right)^2 \\ &= -\kappa \alpha_k^3 \langle U_{0yy}, U_{0yy} \rangle. \end{aligned} \quad (3.52)$$

233 Using the fact that U_{0y} is odd and U_{0yy} is even, we obtain

$$\langle U_{0y}, U_{0yy} \rangle = 0. \quad (3.53)$$

234 Since the inner product between U_{0y} and the even part of \mathcal{F}_3 is 0, we calculate

$$\begin{aligned} \langle \mathcal{F}_3, U_{0y} \rangle &= \left\langle \frac{2V_{2,o}U_0^2V_1 + 2U_{2,o}U_1V_0^2 - 2V_{2,o}U_0U_1V_0 - 2U_{2,o}U_0V_1V_0 - U_0^2V_{3,o}V_0}{V_0^3}, U_{0y} \right\rangle \\ &= c_{k,0}^2 b_{k,2} I_1 - c_{k,0} b_{k,3} I_2, \end{aligned} \quad (3.54)$$

235 where

$$I_1 = \int_{-\infty}^{\infty} 2[(y\rho - f_2)(\rho g_1 - f_1) - g_3 \rho^2] \rho' dy, \quad I_2 = \int_{-\infty}^{\infty} y \rho^2 \rho' dy. \quad (3.55)$$

236 Thus,

$$\frac{\partial \alpha_k}{\partial T_2} = \hat{\tau} \kappa^2 \alpha_k - \frac{\kappa \int_{-\infty}^{\infty} (\rho'')^2 dy}{\int_{-\infty}^{\infty} \rho'^2 dy} \alpha_k^3 - \frac{c_{k,0} b_{k,2} I_1 - b_{k,3} I_2}{c_{k,0} \int_{-\infty}^{\infty} \rho'^2 dy}. \quad (3.56)$$

We summarize the equations for p_k and α_k at the first two time scales as follows:

$$\frac{\partial p_k}{\partial T_1} = \kappa \alpha_k, \quad (3.57a)$$

$$\frac{\partial \alpha_k}{\partial T_1} = \frac{b_{k,2} \int_{-\infty}^{\infty} \rho^2 \rho' y dy}{c_{k,0} \int_{-\infty}^{\infty} \rho'^2 dy}, \quad (3.57b)$$

$$\frac{\partial p_k}{\partial T_2} = \frac{b_{k,2} \int_{-\infty}^{\infty} \rho^2 \rho' y dy}{c_{k,0} \int_{-\infty}^{\infty} \rho'^2 dy} - \frac{c_{k,1} \int_{-\infty}^{\infty} \rho'^2 dy + c_{k,0}^2 \int_{-\infty}^{\infty} f_{1y} \rho' dy}{c_{k,0} \int_{-\infty}^{\infty} \rho'^2 dy} \kappa \alpha_k, \quad (3.57c)$$

$$\frac{\partial \alpha_k}{\partial T_2} = \hat{\tau} \kappa^2 \alpha_k - \frac{\kappa \int_{-\infty}^{\infty} (\rho'')^2 dy}{\int_{-\infty}^{\infty} \rho'^2 dy} \alpha_k^3 - \frac{c_{k,0} b_{k,2} I_1 - b_{k,3} I_2}{c_{k,0} \int_{-\infty}^{\infty} \rho'^2 dy}. \quad (3.57d)$$

Thus, Eq. (3.4) becomes

$$\dot{p}_k = \kappa \alpha_k \varepsilon + \left(\frac{b_{k,2} \int_{-\infty}^{\infty} \rho^2 \rho' y dy}{c_{k,0} \int_{-\infty}^{\infty} \rho'^2 dy} - \frac{c_{k,1} \int_{-\infty}^{\infty} \rho'^2 dy + c_{k,0}^2 \int_{-\infty}^{\infty} f_{1y} \rho' dy}{c_{k,0} \int_{-\infty}^{\infty} \rho'^2 dy} \kappa \alpha_k \right) \varepsilon^2 + \mathcal{O}(\varepsilon^3), \quad (3.58a)$$

$$\dot{\alpha}_k = \frac{b_{k,2} \int_{-\infty}^{\infty} \rho^2 \rho' y dy}{c_{k,0} \int_{-\infty}^{\infty} \rho'^2 dy} \varepsilon + \left(\hat{\tau} \kappa^2 \alpha_k - \frac{\kappa \int_{-\infty}^{\infty} (\rho'')^2 dy}{\int_{-\infty}^{\infty} \rho'^2 dy} \alpha_k^3 - \frac{c_{k,0} b_{k,2} I_1 - b_{k,3} I_2}{c_{k,0} \int_{-\infty}^{\infty} \rho'^2 dy} \right) \varepsilon^2 + \mathcal{O}(\varepsilon^3). \quad (3.58b)$$

237 **Remark 1.** The system (3.58) describes the dynamics of centers of N spikes when our initial condition is close
 238 to the quasi-equilibrium solution, in which $b_{k,2}, b_{k,3}, c_{k,0}$ and $c_{k,1}$ encode the information from other spikes and
 239 need to be determined from the outer solution.

240 **Outer region:** Away from the spike centers where x satisfies $|x - \hat{x}_k| \sim \mathcal{O}(1)$, u is exponentially small and
 241 v satisfies $Dv_{xx} - v \sim 0$ on the interval $x \in [-1, 1]$ with suitable discontinuity conditions imposed across \hat{x}_k . In
 242 the limit $\varepsilon \rightarrow 0$, the even part of $\frac{u^2}{\varepsilon}$ behaves in the distributional sense as a linear combination of $\delta(x - \hat{x}_k)$
 243 for $k = 1, \dots, N$, where $\delta(x)$ is the Dirac delta function. Whereas the odd part of $\frac{u^2}{\varepsilon}$ behaves like a linear
 244 combination of $\delta'(x - \hat{x}_k)$ for $k = 1, \dots, N$. Therefore, v satisfies

$$Dv_{xx} - v + \sum_{k=1}^N (s_k \delta(x - x_k - \varepsilon p_k) + \varepsilon^2 h_k \delta'(x - x_k - \varepsilon p_k)) = 0, \quad v'(\pm 1) = 0, \quad (3.59)$$

245 where

$$\begin{aligned}
s_k &= s_{k,0} + s_{k,1}\varepsilon + \cdots \\
&= \int_{-\infty}^{\infty} U_0^2 dy + \varepsilon \int_{-\infty}^{\infty} 2U_0U_1 dy + \varepsilon^2 \int_{-\infty}^{\infty} (U_1^2 + 2U_0U_{2,e}) dy + \mathcal{O}(\varepsilon^3) \\
&= c_{k,0}^2 \int_{-\infty}^{\infty} \rho^2 dy + \varepsilon \left(2c_{k,0}c_{k,1} \int_{-\infty}^{\infty} \rho^2 dy + 2c_{k,0}^3 \int_{-\infty}^{\infty} \rho f_1 dy \right) + \varepsilon^2 \left(c_{k,1}^2 \int_{-\infty}^{\infty} \rho^2 dy + 2c_{k,1}c_{k,0}^2 \int_{-\infty}^{\infty} \rho f_1 dy \right. \\
&\quad + c_{k,0}^4 \int_{-\infty}^{\infty} f_1^2 dy + 2c_{k,1}c_{k,0}^2 \int_{-\infty}^{\infty} \rho e_1 dy + 2c_{k,2}c_{k,0} \int_{-\infty}^{\infty} \rho^2 dy + 2c_{k,0}^2 \int_{-\infty}^{\infty} (\rho e_2 + \frac{\kappa\alpha_k^2}{2} y\rho\rho') dy \\
&\quad \left. + 2c_{k,0}^4 \int_{-\infty}^{\infty} \rho e_3 dy \right) + \mathcal{O}(\varepsilon^3),
\end{aligned} \tag{3.60}$$

246

$$\begin{aligned}
h_k &= h_{k,0} + \varepsilon h_{k,1} + \cdots \\
&= \int_{-\infty}^{\infty} \int_{-\infty}^z 2U_0U_{2,o} d\hat{y}dz + \mathcal{O}(\varepsilon) \\
&= 2c_{k,0}b_{k,2} \int_{-\infty}^{+\infty} \int_{+\infty}^z \rho f_2 d\hat{y}dz + \mathcal{O}(\varepsilon).
\end{aligned} \tag{3.61}$$

247 Solving Eq. (3.59) yields

$$v = \sum_{k=1}^N s_k G(x; x_k + \varepsilon p_k) - \varepsilon^2 \sum_{k=1}^N h_k G_z(x; x_k + \varepsilon p_k), \tag{3.62}$$

248 where $G(x; z)$ is the Green's function satisfying

$$DG_{xx} - G = -\delta(x - z), \quad G_x(\pm 1) = 0, \tag{3.63}$$

249 and $G_z(x; z)$ is the derivative of Green's function with respect to the second variable, which satisfies

$$DG_{zxx} - G_z = \delta'(x - z), \quad G_{zx}(\pm 1) = 0. \tag{3.64}$$

250 A simple calculation gives:

$$G(x; z) = \frac{1}{\sqrt{D} \sinh(2/\sqrt{D})} \begin{cases} \cosh\left(\frac{1-z}{\sqrt{D}}\right) \cosh\left(\frac{1+x}{\sqrt{D}}\right), & -1 < x < z, \\ \cosh\left(\frac{1+z}{\sqrt{D}}\right) \cosh\left(\frac{1-x}{\sqrt{D}}\right), & z < x < 1. \end{cases} \tag{3.65}$$

251 For convenience, we rewrite G as

$$G = \frac{1}{2\sqrt{D}} e^{-|x-z|/\sqrt{D}} + R(x; z), \tag{3.66}$$

252 where R is the regular part of Green's function. Then, near the k -th spike $x = x_k + \varepsilon(p_k + y)$, we have

$$\begin{aligned}
v(x) &= \sum_{j=1}^N s_j G(x_k + \varepsilon y + \varepsilon p_k; x_j + \varepsilon p_j) - \varepsilon^2 \sum_{j=1}^N h_j G_z(x_k + \varepsilon y + \varepsilon p_k; x_j + \varepsilon p_j) \\
&= v_{k,0}(y) + \varepsilon v_{k,1}(y) + \varepsilon^2 v_{k,2}(y) + \varepsilon^3 v_{k,3}(y) + \cdots
\end{aligned} \tag{3.67}$$

where

$$v_{k,0} = \sum_{j=1}^N s_{j,0} G(x_k; x_j), \tag{3.68}$$

$$v_{k,1} = \sum_{j=1}^N s_{j,1} G(x_k; x_j) + \sum_{j=1}^N s_{j,0} [G_x(x_k; x_j)p_k + G_z(x_k; x_j)p_j] + y \sum_{j=1}^N s_{j,0} G_x(x_k^\pm; x_j). \tag{3.69}$$

Since only the derivatives of $v_{k,2}$ and $v_{k,3}$ at $y = 0$ are needed in the later matching procedure, we compute $\frac{\partial v_{k,2}(0^\pm)}{\partial y}$ and $\frac{\partial v_{k,3}(0^\pm)}{\partial y}$ as follows,

$$\frac{\partial v_{k,2}(0^\pm)}{\partial y} = \sum_{j=1}^N (s_{j,0} [G_{xx}(x_k^\pm; x_j)p_k + G_{zx}(x_k^\pm; x_j)p_j] + s_{j,1} G_x(x_k^\pm; x_j)), \tag{3.70}$$

$$\begin{aligned}
\frac{\partial v_{k,3}(0^\pm)}{\partial y} &= \sum_{j=1}^N \left(\frac{1}{6} s_{j,0} [3G_{xxx}(x_k^\pm; x_j)p_k^2 + 6G_{zxx}(x_k^\pm; x_j)p_k p_j + 3G_{zzx}(x_k^\pm; x_j)p_j^2] \right. \\
&\quad \left. + s_{j,1} [G_{xx}(x_k^\pm; x_j)p_k + G_{zx}(x_k^\pm; x_j)p_j] + s_{j,2} G_x(x_k^\pm; x_j) - h_{j,0} G_{zx}(x_k^\pm; x_j) \right).
\end{aligned} \tag{3.71}$$

253 **Matching:** To determine the constants in the inner region, we match the local behavior of the solution v
 254 with the far field behavior of V in each order of ε . For convenience, we define the matrix \mathcal{G} as

$$\mathcal{G} = (G(x_k; x_j)). \quad (3.72)$$

255 Let us denote $\frac{\partial}{\partial x_k}$ as ∇_{x_k} . When $k \neq j$, we can define $\nabla_{x_k} G(x_k; x_j)$ and $\nabla_{x_j} G(x_k; x_j)$ in the classical way. When
 256 $k = j$, we define

$$\nabla_{x_k} G(x_k; x_k) := \frac{\partial}{\partial x} \Big|_{x=x_k} R(x; x_k). \quad (3.73)$$

257 We also define the matrix \mathcal{P} and \mathcal{G}_g as follows,

$$\mathcal{P} := (\nabla_{x_k} G(x_k; x_j)), \quad (3.74)$$

258

$$\mathcal{G}_g := (\nabla_{x_j} \nabla_{x_k} G(x_k; x_j)). \quad (3.75)$$

259 As we have chosen x_k as the equilibrium position of the k -th spike, we have the following identities related to G
 260 from [7]:

$$\sum_{j=1}^N G(x_k; x_j) = c_g, \quad (3.76a)$$

261

$$\sum_{j=1}^N \nabla_{x_k} G(x_k; x_j) = 0, \quad \sum_{k=1}^N \nabla_{x_j} G(x_k; x_j) = 0, \quad \nabla_{x_k} G(x_k; x_j) = \nabla_{x_k} G(x_j; x_k). \quad (3.76b)$$

262 where $c_g := \left[2\sqrt{D} \tanh\left(\frac{1}{\sqrt{D}N}\right) \right]^{-1}$ is a constant independent of k .

263 Matching the term in the leading order, we obtain

$$c_{k,0} = \sum_{j=1}^N s_{j,0} G(x_k; x_j). \quad (3.77)$$

264 We assume N spikes have the same height in the leading order, then $c_{k,0}$ has the same value for $k = 1, \dots, N$.
 265 Using Eq. (3.76a), we solve Eq. (3.77) to obtain

$$c_{k,0} = \frac{1}{c_g \int_{-\infty}^{\infty} \rho^2 dy}. \quad (3.78)$$

266 Matching the terms in the order ε , we obtain

$$b_{k,1} = \frac{1}{2} (V_1'(+\infty) + V_1'(-\infty)) = \frac{1}{2} \left(\frac{\partial v_{k,1}(0^+)}{\partial y} + \frac{\partial v_{k,1}(0^-)}{\partial y} \right) = \sum_{j=1}^N s_{j,0} \nabla_{x_k} G(x_k; x_j), \quad (3.79)$$

267 and

$$\begin{aligned} c_{k,1} &= v_{k,1}(0) + \frac{c_{k,0}^2}{D} \int_0^{+\infty} \int_{+\infty}^y \rho^2 dz dy \\ &= \sum_{j=1}^N s_{j,1} G(x_k; x_j) + \sum_{j=1}^N s_{j,0} [\nabla_{x_k} G(x_k; x_j) p_k + \nabla_{x_j} G(x_k; x_j) p_j] + \frac{c_{k,0}^2}{D} \int_0^{+\infty} \int_{+\infty}^y \rho^2 dz dy. \end{aligned} \quad (3.80)$$

268 Substituting Eq. (3.76b) into Eq. (3.79), we obtain

$$b_{k,1} = 0, \quad (3.81)$$

269 which is in consistent with the solvability condition Eq. (3.20) in the inner region. Using Eq. (3.76a) and
 270 Eq. (3.76b), we can rewrite Eq. (3.80) in the form

$$\left(-\frac{2}{c_g} \mathcal{G} + \mathcal{I} \right) \mathbf{c}_1 = \frac{1}{c_g^2 \int_{-\infty}^{\infty} \rho^2 dy} (\mathcal{P}^\top \mathbf{p} + \tilde{c} \mathbf{1}_N), \quad (3.82)$$

271 where \mathcal{I} is the identity matrix, $\mathbf{p} := [p_1, p_2, \dots, p_N]^\top$, $\mathbf{c}_1 := [c_{1,1}, c_{2,1}, \dots, c_{N,1}]^\top$, $\mathbf{1}_N = [1, 1, \dots, 1]^\top$ and

$$\tilde{c} = \left(\int_{-\infty}^{+\infty} \rho^2 dy \right)^{-1} \left(\frac{1}{D} \int_0^{+\infty} \int_{+\infty}^y \rho^2 dz dy + 2 \left(\int_{-\infty}^{+\infty} \rho^2 dy \right)^{-1} \int_{-\infty}^{+\infty} \rho f_1 dy \right). \quad (3.83)$$

272 Using $\left(-\frac{2}{c_g}\mathcal{G} + \mathcal{I}\right)^{-1} \mathbf{1}_N = -\mathbf{1}_N$, we can express \mathbf{c}_1 as

$$\mathbf{c}_1 = \frac{1}{c_g^2 \int_{-\infty}^{\infty} \rho^2 dy} \left(\left(-\frac{2}{c_g}\mathcal{G} + \mathcal{I} \right)^{-1} \mathcal{P}^\top \mathbf{p} - \bar{c} \mathbf{1}_N \right). \quad (3.84)$$

273 Matching the terms in the order of ε^2 , we obtain

$$\begin{aligned} b_{k,2} &= \frac{1}{2} (V_2'(+\infty) + V_2'(-\infty)) \\ &= \frac{1}{2} \left(\frac{\partial v_{k,2}(0^+)}{\partial y} + \frac{\partial v_{k,2}(0^-)}{\partial y} \right) \\ &= \sum_{j=1}^N (s_{j,0} [\nabla_{x_k} \nabla_{x_k} G(x_k; x_j) p_k + \nabla_{x_j} \nabla_{x_k} G(x_k; x_j) p_j] + s_{j,1} \nabla_{x_k} G(x_k; x_j)). \end{aligned} \quad (3.85)$$

274 Using the fact that $\sum_{j=1}^N \nabla_{x_k} \nabla_{x_k} G(x_k; x_j) = \frac{1}{D} \sum_{j=1}^N G(x_k; x_j) = \frac{c_g}{D}$ and $\mathcal{P} \mathbf{1}_N = 0$, Eq. (3.85) becomes

$$\begin{aligned} \mathbf{b}_2 &= \frac{1}{c_g^2 \int_{-\infty}^{\infty} \rho^2 dy} \left(\frac{c_g}{D} \mathcal{I} + \mathcal{G}_g \right) \mathbf{p} + \frac{2}{c_g} \mathcal{P} \mathbf{c}_1 \\ &= \frac{1}{c_g^2 \int_{-\infty}^{\infty} \rho^2 dy} \left(\frac{c_g}{D} \mathcal{I} + \mathcal{G}_g + \frac{2}{c_g} \mathcal{P} \left(-\frac{2}{c_g}\mathcal{G} + \mathcal{I} \right)^{-1} \mathcal{P}^\top \right) \mathbf{p}. \end{aligned} \quad (3.86)$$

275 Matching the constant terms in the order of ε^2 , we obtain

$$\begin{aligned} c_{k,2} &= \frac{1}{2} \sum_{j=1}^N s_{j,0} [\nabla_{x_k} \nabla_{x_k} G(x_k; x_j) p_k^2 + 2 \nabla_{x_k} \nabla_{x_j} G(x_k; x_j) p_k p_j + \nabla_{x_j} \nabla_{x_j} G(x_k; x_j) p_j^2] \\ &\quad + \sum_{j=1}^N s_{j,1} [\nabla_{x_k} G(x_k; x_j) p_k + \nabla_{x_j} G(x_k; x_j) p_j] + \sum_{j=1}^N s_{j,2} G(x_k; x_j) + \frac{2c_{k,0}c_{k,1}}{D} \int_0^{+\infty} \int_{+\infty}^y \rho^2 dz dy \\ &\quad + \frac{2c_{k,0}^3}{D} \int_0^{+\infty} \int_{+\infty}^y \rho f_1 dz dy. \end{aligned} \quad (3.87)$$

276 Matching the terms in the order of ε^3 , we obtain

$$\begin{aligned} b_{k,3} &= \frac{1}{2} (V_3'(+\infty) + V_3'(-\infty)) + \frac{2c_{k,0}b_{k,2}}{D} \int_0^{\infty} \rho f_2 dy \\ &= \frac{1}{2} \left(\frac{\partial v_{k,3}(0^+)}{\partial y} + \frac{\partial v_{k,3}(0^-)}{\partial y} \right) + \frac{2c_{k,0}b_{k,2}}{D} \int_0^{\infty} \rho f_2 dy \\ &= \sum_{j=1}^N \left(\frac{1}{2} s_{j,0} [\nabla_{x_k} \nabla_{x_k} \nabla_{x_k} G(x_k; x_j) p_k^2 + 2 \nabla_{x_j} \nabla_{x_k} \nabla_{x_k} G(x_k; x_j) p_k p_j + \nabla_{x_j} \nabla_{x_j} \nabla_{x_k} G(x_k; x_j) p_j^2] \right. \\ &\quad \left. + s_{j,1} [\nabla_{x_k} \nabla_{x_k} G(x_k; x_j) p_k + \nabla_{x_j} \nabla_{x_k} G(x_k; x_j) p_j] + s_{j,2} \nabla_{x_k} G(x_k; x_j) - h_{j,0} \nabla_{x_j} \nabla_{x_k} G(x_k^\pm; x_j) \right) \\ &\quad + \frac{2c_{k,0}b_{k,2}}{D} \int_0^{\infty} \rho f_2 dy. \end{aligned} \quad (3.88)$$

277 Observe that $c_{k,2}$ and $b_{k,3}$ consist of quadratic terms and linear terms involving p_j , $j = 1, \dots, N$, which will
278 be eliminated in determining the ODE for the slow evolution of the amplitude in the later subsection. Hence, we
279 omit the exact evaluations of them.

280 The constants in Eq. (3.58) have been determined explicitly. Thus, the dynamics of spikes' centers in the
281 vicinity of Hopf bifurcations is governed by the system (3.58), where the constants $c_{k,0}$, $c_{k,1}$, $c_{k,2}$, $b_{k,1}$, $b_{k,2}$, $b_{k,3}$
282 are determined by Eqs. (3.78) (3.84) (3.87) (3.81) (3.86) and (3.88). We do not intend to solve the full system
283 but seek a leading order approximation in the order of ε .

284 3.2 Leading order periodic solution

285 Eq. (3.58) can be seen as a linear system with weakly nonlinear parts. We proceed to determine the leading order
286 dynamics of Eq. (3.58). We denote

$$\mathcal{M} = \frac{c_g}{D} \mathcal{I} + \mathcal{G}_g + \frac{2}{c_g} \mathcal{P} \left(-\frac{2}{c_g}\mathcal{G} + \mathcal{I} \right)^{-1} \mathcal{P}^\top. \quad (3.89)$$

287 Substituting Eq. (3.58a) into Eq. (3.58b) and using the slow time $t_1 = \varepsilon t$, we can obtain a second order nonlinear
 288 ODE system:

$$\frac{d^2 \mathbf{p}}{dt_1^2} - \kappa \beta_1 \mathcal{M} \mathbf{p} = \varepsilon \left((\hat{\tau} \kappa^2 \mathcal{I} + \beta_1 \mathcal{M}) \frac{d\mathbf{p}}{dt_1} - \frac{\beta_2}{\kappa} \left(\frac{d\mathbf{p}}{dt_1} \right)^{\circ 3} + \frac{d\mathbf{F}}{dt_1} + \mathbf{H} \right), \quad (3.90)$$

289 where $[\sim]^{\circ 3}$ is the Hadamard power, β_1 and β_2 are constants

$$\beta_1 := \frac{\int_{-\infty}^{\infty} \rho^2 \rho' y \, dy}{c_g \int_{-\infty}^{\infty} \rho'^2 \, dy} = -\frac{2}{c_g}, \quad \beta_2 := \frac{\int_{-\infty}^{\infty} (\rho'')^2 \, dy}{\int_{-\infty}^{\infty} \rho'^2 \, dy} = \frac{5}{7}, \quad (3.91)$$

290 $\mathbf{F} \left(\mathbf{p}, \frac{d\mathbf{p}}{dt_1} \right)$ and $\mathbf{H} \left(\mathbf{p}, \frac{d\mathbf{p}}{dt_1} \right)$ are vectors defined as

$$\mathbf{F} = \begin{bmatrix} F_1 \\ F_2 \\ \vdots \\ F_N \end{bmatrix}, \quad \mathbf{H} = \begin{bmatrix} H_1 \\ H_2 \\ \vdots \\ H_N \end{bmatrix}, \quad (3.92)$$

291 with

$$F_k = -\frac{c_{k,1} \int_{-\infty}^{\infty} \rho'^2 \, dy + c_{k,0}^2 \int_{-\infty}^{\infty} f_{1y} \rho' \, dy}{c_{k,0} \int_{-\infty}^{\infty} \rho'^2 \, dy} \kappa \alpha_k, \quad H_k = -\kappa \frac{c_{k,0} b_{k,2} I_1 - b_{k,3} I_2}{c_{k,0} \int_{-\infty}^{\infty} \rho'^2 \, dy}. \quad (3.93)$$

292 The eigenvalues of the matrix \mathcal{M} are crucial to determine the dynamics. In [7] (see Eq. (4.58)), the eigenvalues
 293 and eigenvectors of \mathcal{M} are computed analytically. We summarize the result as follows:

294 **Lemma 1.** *The eigenvalue ζ_k of \mathcal{M} are*

$$\zeta_k = \frac{c_g}{D} - \frac{1}{D^{\frac{3}{2}} \nu_k} + \frac{2}{D^{\frac{3}{2}} \nu_k (c_g \sqrt{D} \nu_k - 2)} \operatorname{csch}^2 \left(\frac{2}{\sqrt{DN}} \right) \sin^2 \left(\frac{\pi k}{N} \right), \quad (3.94)$$

295 with $\nu_k = 2 \coth \left(\frac{2}{\sqrt{DN}} \right) - 2 \operatorname{csch} \left(\frac{2}{\sqrt{DN}} \right) \cos \left(\frac{\pi k}{N} \right)$ and the associated normalized eigenvectors \mathbf{q}_k of \mathcal{M} are defined
 296 in Eq. (2.11). These eigenvalues are positive and ordered as $\zeta_N > \dots > \zeta_2 > \zeta_1 > 0$ only when $D < D_N^*$, where

$$D_N^* := \frac{1}{N^2 \ln^2 (1 + \sqrt{2})}. \quad (3.95)$$

297 **Remark 2.** *The terms $\frac{c_g}{D}$, $-\frac{1}{D^{\frac{3}{2}} \nu_k}$, and $\frac{2}{D^{\frac{3}{2}} \nu_k (c_g \sqrt{D} \nu_k - 2)} \operatorname{csch}^2 \left(\frac{2}{\sqrt{DN}} \right) \sin^2 \left(\frac{\pi k}{N} \right)$ are eigenvalues of the matrices
 298 $\frac{c_g}{D} \mathcal{I}$, \mathcal{G}_g , and $\frac{2}{c_g} \mathcal{P} \left(-\frac{2}{c_g} \mathcal{G} + \mathcal{I} \right)^{-1} \mathcal{P}^\top$, respectively. The order of ζ_k when $D < D_N^*$ is not mentioned in the
 299 reference [7], but we can see it by further simplifying ζ_k as*

$$\zeta_k = \frac{c_g}{D} \frac{(1 - \cos \left(\frac{k\pi}{N} \right)) \left(1 - 2 \tanh^2 \left(\frac{1}{\sqrt{DN}} \right) \right)}{2 - \cosh \left(\frac{2}{\sqrt{DN}} \right) - \cos \left(\frac{k\pi}{N} \right)}. \quad (3.96)$$

300 Note that D_N^* corresponds to the zero of the term $\left(1 - 2 \tanh^2 \left(\frac{1}{\sqrt{DN}} \right) \right)$.

301 **Remark 3.** *An N -spike equilibrium solution will be stable only when $D < D_N^*$. As we assume N -spike equilibria
 302 are stable at $\tau = 0$, the condition $D < D_N^*$ is implicitly required.*

303 Let $\boldsymbol{\xi} = Q^\top \mathbf{p}$, then Eq. (3.90) becomes

$$\frac{d^2 \boldsymbol{\xi}}{dt_1^2} - \kappa \beta_1 \Lambda \boldsymbol{\xi} = \varepsilon \left((\hat{\tau} \kappa^2 \mathcal{I} + \beta_1 \Lambda) \frac{d\boldsymbol{\xi}}{dt_1} - \frac{\beta_2}{\kappa} Q^\top \left(Q \frac{d\boldsymbol{\xi}}{dt_1} \right)^{\circ 3} + Q^\top \frac{d\mathbf{F} \left(Q \boldsymbol{\xi}, Q \frac{d\boldsymbol{\xi}}{dt_1} \right)}{dt_1} + Q^\top \mathbf{H} \left(Q \boldsymbol{\xi}, Q \frac{d\boldsymbol{\xi}}{dt_1} \right) \right), \quad (3.97)$$

304 where Λ is the diagonal matrix with ζ_k on its diagonal. Next, we derive a multiple-scale approximation of the
 305 solution to Eq. (3.97). We introduce slow time scales $t_2 = \varepsilon t_1$ and assume

$$\boldsymbol{\xi} = \boldsymbol{\xi}_0(t_1, t_2) + \varepsilon \boldsymbol{\xi}_1(t_1, t_2) + \dots. \quad (3.98)$$

306 Then,

$$\frac{d\boldsymbol{\xi}}{dt_1} = \frac{\partial \boldsymbol{\xi}_0}{\partial t_1} + \varepsilon \left(\frac{\partial \boldsymbol{\xi}_1}{\partial t_1} + \frac{\partial \boldsymbol{\xi}_0}{\partial t_2} \right) + \mathcal{O}(\varepsilon^2). \quad (3.99)$$

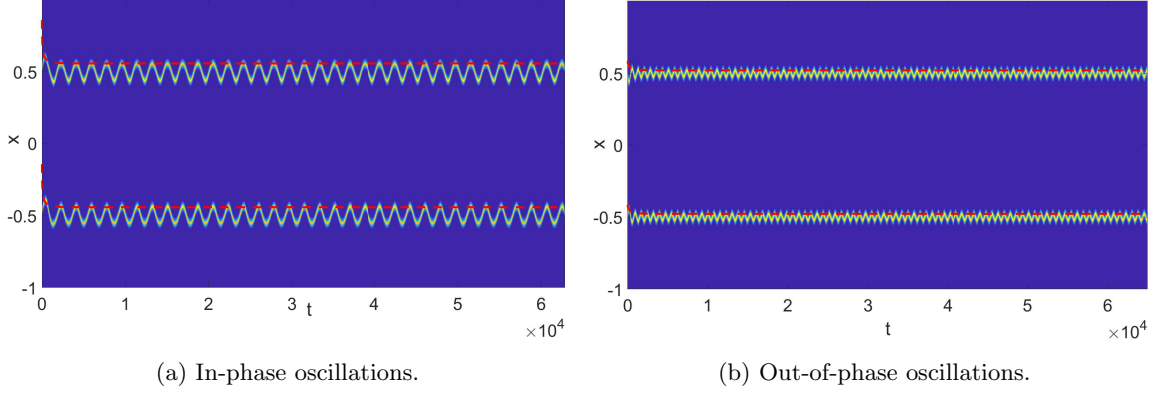


Figure 2: Two types of oscillations in GM model when τ is well beyond $\frac{1}{\kappa}$. The parameters are $\hat{\tau} = 300$, $\varepsilon = 0.01$, $D = \frac{0.2}{\ln^2(1+\sqrt{2})}$, $\kappa = 0.2$. The red dashed lines are the amplitudes' evolution obtained from solving the system (3.104). The only difference between Fig. 2a and Fig. 2b is the initial condition we select.

307 Substituting Eq. (3.98) into Eq. (3.97) and collecting terms in the leading order yield

$$\frac{\partial^2 \xi_0}{\partial t_1^2} - \kappa \beta_1 \Lambda \xi_0 = 0. \quad (3.100)$$

308 The general solution of this problem is

$$\xi_0 = \begin{bmatrix} B_1(t_2) \cos(\omega_1 t_1 + \theta_1(t_2)) \\ B_2(t_2) \cos(\omega_2 t_1 + \theta_2(t_2)) \\ \vdots \\ B_N(t_2) \cos(\omega_N t_1 + \theta_N(t_2)) \end{bmatrix}, \quad (3.101)$$

309 where

$$\omega_k = \sqrt{-\kappa \beta_1 \zeta_k}, \quad (3.102)$$

$B_k(t_2)$ and $\theta_k(t_2)$ are functions of slow time scale t_2 that need to be determined in the $\mathcal{O}(\varepsilon)$ equation. In the order of ε , we have

$$\begin{aligned} \frac{\partial^2 \xi_1}{\partial t_1^2} - \kappa \beta_1 \Lambda \xi_1 = & -2 \frac{\partial^2 \xi_0}{\partial t_1 \partial t_2} \\ & + \left((\hat{\tau} \kappa^2 \mathcal{I} + \beta_1 \Lambda) \frac{\partial \xi_0}{\partial t_1} - \frac{\beta_2}{\kappa} Q^\top \left(Q \frac{\partial \xi_0}{\partial t_1} \right)^{\circ 3} + Q^\top \frac{\partial \mathbf{F}}{\partial t_1} \left(Q \xi_0, Q \frac{\partial \xi_0}{\partial t_1} \right) + Q^\top \mathbf{H} \left(Q \xi_0, Q \frac{\partial \xi_0}{\partial t_1} \right) \right). \end{aligned} \quad (3.103)$$

310 Note that Eq. (3.103) can be decoupled into N independent second order inhomogeneous ODEs. To obtain a
 311 bounded solution for each element of ξ_1 , we need to remove the secular terms (the solutions of the associated
 312 homogeneous equation) in the inhomogeneous part. A careful examination shows that $Q^\top \frac{\partial \mathbf{F}}{\partial t_1} \left(Q \xi_0, Q \frac{\partial \xi_0}{\partial t_1} \right)$ and
 313 $Q^\top \mathbf{H} \left(Q \xi_0, Q \frac{\partial \xi_0}{\partial t_1} \right)$ contain no secular terms involving $\sin(\omega_k t_1 + \theta_k(t_2))$ in the k -th component of Eq. (3.103).
 314 Then, by removing the secular term involving $\sin(\omega_k t_1 + \theta_k(t_2))$ in the k -th component, we obtain the equations
 315 for the amplitude of $\xi_{0,k}$

$$\frac{dB_k}{dt_2} = B_k \left[\frac{1}{2} (\hat{\tau} \kappa^2 + \beta_1 \zeta_k) - \frac{3\beta_2}{8\kappa N} \sum_{j=1}^N a_{k,j} \omega_j^2 B_j^2 \right], \quad (3.104)$$

316 where

$$a_{k,j} = \begin{cases} N \sum_{l=1}^N Q_{lj}^4 & j = k \\ 2N \sum_{l=1}^N Q_{lj}^2 Q_{lk}^2 & j \neq k \end{cases}. \quad (3.105)$$

317 **Remark 4.** We can obtain the equation of $\theta_k(t_2)$ by removing the secular terms involving $\cos(\omega_k t_1 + \theta_k(t_2))$ in
 318 the k -th component of Eq. (3.103). In this situation, \mathbf{F} and \mathbf{H} will contribute to the secular term. As we are
 319 interested in the amplitude system that is critical to the manifestation of the periodic orbit, we will not go into
 320 details here.

321 **Remark 5.** Note that $\beta_1 \zeta_k$ are the eigenvalues of the system at $\tau = 0$. Hence, the system Eq. (3.104) is the
 322 same as the corresponding amplitude equations for the extended Schnakenberg model in [27] except the different
 323 constants terms.

324 We summarize our results as follows,

325 **Principal Result 1.** Let

$$\tau = \frac{1}{\kappa} + \varepsilon^2 \hat{\tau},$$

326 and assume that $\hat{\tau} = O(1)$ as $\varepsilon \rightarrow 0$. Then there exists a solution to the extended Gierer-Meinhardt system (3.1)
 327 consisting of N spikes nearly-uniformly spaced, but whose centers evolve near the symmetric configurations on a
 328 slow time-scale according to the following. Let \hat{x}_k be the center of the k -th spike. Then $\hat{x}_k \sim -1 + \frac{2k-1}{N} + \varepsilon p_k$
 329 where

$$p_k = \sum_{j=1}^N Q_{kj} B_j(\varepsilon^2 t) \cos(\varepsilon \omega_j t + \theta_j(\varepsilon^2 t)). \quad (3.106)$$

330 In Eq. (3.106), Q_{kj} is the entry of the matrix Q defined by Eq. (2.10), ω_j is defined by Eq. (3.102) and the
 331 associated amplitudes $\{B_j(s), j = 1, \dots, N\}$ satisfy Eq. (3.104).

332 3.3 Amplitude equations for the extended Gray-Scott model

333 We consider the extended Gray-Scott system:

$$\begin{cases} u_t = \varepsilon^2 u_{xx} - (1 - \kappa)u + Au^2v - \kappa w, \\ 0 = Dv_{xx} + 1 - v - \frac{u^2v}{\varepsilon}, \\ \tau w_t = u - w, \\ \text{Neumann boundary conditions at } x = \pm 1. \end{cases} \quad (3.107)$$

334 It has been shown in [15] that there are two symmetric N -spike equilibrium solutions to the system (3.107) at
 335 $\tau = 0$ given asymptotically by

$$u_{\pm}(x) \sim \frac{1}{AV_{\pm}} \sum_{j=1}^N \rho(\varepsilon^{-1}(x - x_j)), \quad v_{\pm}(x) \sim 1 - \frac{1 - V_{\pm}}{c_g} \sum_{j=1}^N G(x, x_j), \quad (3.108)$$

336 where

$$V_{\pm} = \frac{1}{2} \left(1 \pm \sqrt{1 - 24c_g/A^2} \right), \quad (3.109)$$

337 with $c_g := \left[2\sqrt{D} \tanh\left(\frac{1}{\sqrt{D}N}\right) \right]^{-1}$ defined in Eq. (3.76a). A necessary condition to have an N -spike solution is

$$c_g < \frac{A^2}{24}, \quad (3.110)$$

338 which implicitly poses a restriction on D . The stability analysis of these two symmetric N -spike equilibrium
 339 solutions of two-component system in [15] further reveals that the solution contains V_+ is always unstable to the
 340 small eigenvalues when $N > 1$. As to the solution determined by V_- , we have the following lemma related to the
 341 stability of an N -spike equilibrium solution at $\tau = 0$, see Proposition 3.3 in [15].

342 **Lemma 2.** An N -spike equilibrium solution is stable at $\tau = 0$ if D satisfies the following transcendental equation

$$D < \frac{4}{N^2 \ln^2 \left(\frac{s_g+1}{s_g-1} + \sqrt{\left(\frac{s_g+1}{s_g-1}\right)^2 - 1} \right)}, \quad (3.111)$$

343 where

$$s_g := \frac{1 - V_-}{V_-}. \quad (3.112)$$

344 Now we start to derive the dynamics of spikes near the Hopf bifurcations. The inner region analysis of
 345 the Gray-Scott model is similar to the Schnakenberg model, while the outer solution has the same structure as
 346 the Gierer-Meinhardt model up to a constant addend. After a tedious but straightforward analysis as we have
 347 done for the extended Gierer-Meinhardt model, we obtain the following equations for the slow evolution of the
 348 amplitudes:

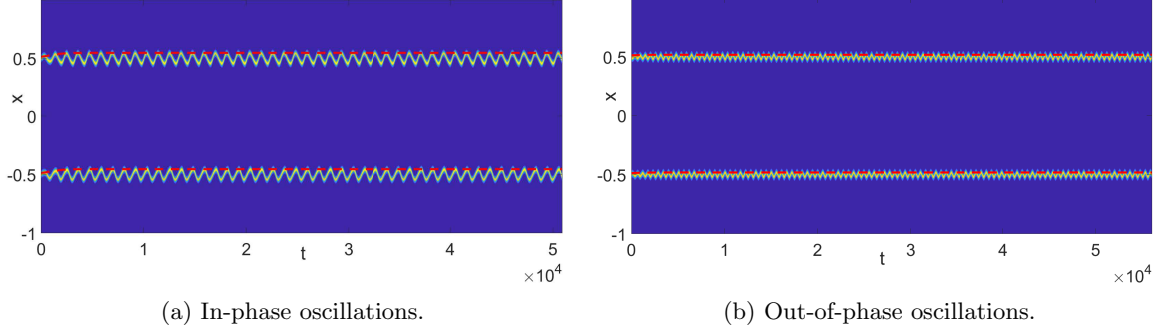


Figure 3: Two types of oscillations in GS model when τ is well beyond $\frac{1}{\kappa}$. The parameters are $\hat{\tau} = 450$, $\varepsilon = 0.01$, $D = 0.2$, $\kappa = 0.2$, $A = 6$. The red dashed lines are the amplitudes' evolution obtained from solving the system (3.113a). The difference between Fig. 3a and Fig. 3b is the initial conditions we select.

$$\frac{dB_k}{dt_2} = B_k \left[\frac{1}{2}(\hat{\tau}\kappa^2 + \beta_1\zeta_k) - \frac{3\beta_2}{8\kappa N} \sum_{j=1}^N a_{k,j}\omega_j^2 B_j^2 \right], \quad (3.113a)$$

349 where

$$a_{k,j} = \begin{cases} N \sum_{l=1}^N Q_{lj}^4 & j = k \\ 2N \sum_{l=1}^N Q_{lj}^2 Q_{lk}^2 & j \neq k \end{cases}, \quad (3.113b)$$

350 and

$$\beta_1 := \frac{s_g \int_{-\infty}^{\infty} \rho^2 \rho' y \, dy}{c_g \int_{-\infty}^{\infty} \rho'^2 \, dy} = -\frac{2s_g}{c_g}, \quad \beta_2 := \frac{\int_{-\infty}^{\infty} (\rho'')^2 \, dy}{\int_{-\infty}^{\infty} \rho'^2 \, dy} = \frac{5}{7}, \quad \omega_k = \sqrt{-\kappa\beta_1\zeta_k}. \quad (3.113c)$$

351 The matrix Q is defined the same as Eq. (2.10), and ζ_k , $k = 1, \dots, N$ (with abuse of notations) are eigenvalues
352 of

$$\mathcal{M} = \frac{c_g}{D} \mathcal{I} + \mathcal{G}_g + \frac{s_g}{c_g} \mathcal{P} \left(-\frac{s_g}{c_g} \mathcal{G} + \mathcal{I} \right)^{-1} \mathcal{P}^\top, \quad (3.114)$$

353 which can be computed as

$$\zeta_k = \frac{c_g}{D} - \frac{1}{D^{\frac{3}{2}} \nu_k} + \frac{s_g}{D^{\frac{3}{2}} \nu_k (c_g \sqrt{D} \nu_k - s_g)} \operatorname{csch}^2 \left(\frac{2}{\sqrt{DN}} \right) \sin^2 \left(\frac{\pi k}{N} \right). \quad (3.115)$$

354 Then, we arrive at the following result:

355 **Principal Result 2.** *Let*

$$\tau = \frac{1}{\kappa} + \varepsilon^2 \hat{\tau},$$

356 *and assume that $\hat{\tau} = O(1)$ as $\varepsilon \rightarrow 0$. Then there exists a solution to the extended Gray-Scott system (3.107)*
357 *consisting of N spikes nearly-uniformly spaced, but whose centers evolve near the symmetric configurations on a*
358 *slow time-scale according to the following. Let \hat{x}_k be the center of the k -th spike. Then $\hat{x}_k \sim -1 + \frac{2k-1}{N} + \varepsilon p_k$*
359 *where*

$$p_k = \sum_{j=1}^N Q_{kj} B_j(\varepsilon^2 t) \cos(\varepsilon \omega_j t + \theta_j(\varepsilon^2 t)). \quad (3.116)$$

360 *In Eq. (3.116), Q_{kj} is the entry of the matrix Q defined by Eq. (2.10), ω_j is defined by (3.113c) and the associated*
361 *amplitudes $\{B_j(s), j = 1, \dots, N\}$ satisfy Eq. (3.113a).*

3.4 Numerical Validation

363 In this subsection we use finite element solver FlexPDE7 [28] to numerically solve systems (3.1) and (3.107). In
364 particular, we validate the reduced systems for the amplitude evolutions in the case of two spikes, as predicted
365 in Principal Results 1 and 2.

366 We first outline our procedures. Initial two-spike equilibrium states for which we will use to test the dynamics
367 are obtained by initializing a two-bump pattern in (3.1) and (3.107) with τ set well below the Hopf threshold
368 $\frac{1}{\kappa}$. We then evolve (3.1) and (3.107) until the time t is sufficiently large that changes in solution are no longer

369 observed. Using this equilibrium solution plus a perturbation $[0, 0, \alpha_1 \varepsilon^2 u_{cx}(\frac{x+0.5}{\varepsilon}) + \alpha_2 \varepsilon^2 u_{cx}(\frac{x-0.5}{\varepsilon})]^\top$ as the
 370 initial condition, we increase τ to $\frac{1}{\kappa} + \hat{\tau} \varepsilon^2$ and trial various of values of α_1 and α_2 to test the sluggish dynamics
 371 of (3.104) and (3.113a) near the Hopf bifurcation. Here u_c denotes a single spike solution and $[\alpha_1, \alpha_2]$ gives the
 372 initial moving directions of two spikes.

373 Fig. 2 and Fig. 3 illustrate the coexistence of in-phase and out-of-phase oscillations predicted by (3.104) and
 374 (3.113a). All parameters in the specific system are the same. In Fig. 2a and Fig 3a, the initial perturbation is
 375 chosen as $[\alpha_1, \alpha_2] = [1, 1]$, resulting in in-phase oscillations. In Fig. 2b and Fig 3b, the initial perturbation is chosen
 376 as $[\alpha_1, \alpha_2] = [1, -1]$, resulting in out-of-phase oscillations. The evolution of the amplitudes described by (3.104)
 377 and (3.113a) are solved with Matlab subroutine ODE45 and the results are in good agreement with the full PDE
 378 simulations.

379 4 Stability of equilibria of the amplitude equations

380 In this section, we investigate the equilibrium points of the amplitude equations and their stability, which is
 381 crucial to understand the stable oscillations in the original reaction-diffusion systems. We start with the general
 382 form of amplitude equations

$$\frac{dB_k}{dt_2} = B_k \left[\frac{1}{2}(\hat{\tau}\kappa^2 + \beta_1\zeta_k) - \frac{3\beta_2}{8\kappa N} \sum_{j=1}^N a_{k,j} \omega_j^2 B_j^2 \right], \quad (4.1)$$

383 We introduce new variable $X_k = \frac{3\beta_2}{8\kappa N} \omega_k^2 B_k^2$. Then, the system Eq. (4.1) is equivalent to

$$\frac{dX_k}{dt_2} = 2X_k(\tilde{\tau}_k - \sum_{j=1}^N a_{k,j} X_j), \quad \text{with } X_k \geq 0. \quad (4.2)$$

384 where $\tilde{\tau}_k = \frac{1}{2}(\hat{\tau}\kappa^2 + \beta_1\zeta_k)$. Note that $\tilde{\tau}_k$ is ranked in a descending order, namely, $\tilde{\tau}_1 > \tilde{\tau}_2 > \dots > \tilde{\tau}_N$. In the
 385 following analysis, we will always assume $\tilde{\tau}_N > 0$ such that N Hopf modes are excited.

386 Denote $\mathcal{A}^{(N)}$ as the $N \times N$ matrix with entries $a_{k,j}$. In Appendix A, we calculate $a_{k,j}$ explicitly and have
 387 the following result:

388 **Lemma 3.** For the matrix $\mathcal{A}^{(N)}$,

- 389 • when $N = 2n + 1$, we have

$$a_{k,j} = \begin{cases} 1, & k = j = N, \\ \frac{3}{2}, & k = j \neq N, \\ 1, & k + j = N, \\ 2, & \text{else.} \end{cases} \quad \det \mathcal{A}^{(N)} = \frac{8n+3}{3} \left(-\frac{3}{4}\right)^n, \quad (4.3)$$

- 390 • when $N = 2n$, we have

$$a_{k,j} = \begin{cases} 1, & k = j = N \quad \text{and} \quad k = j = n, \\ \frac{3}{2}, & k = j \neq N \quad \text{and} \quad k = j \neq n, \\ 1, & k + j = N, \\ 2, & \text{else.} \end{cases} \quad \det \mathcal{A}^{(N)} = -\frac{8n+1}{3} \left(-\frac{3}{4}\right)^{n-1}. \quad (4.4)$$

391 For concreteness, when $N = 5$ and $N = 6$, we have

$$\mathcal{A}^{(5)} = \begin{pmatrix} \frac{3}{2} & 2 & 2 & 1 & 2 \\ 2 & \frac{3}{2} & 1 & 2 & 2 \\ 2 & 1 & \frac{3}{2} & 2 & 2 \\ 1 & 2 & 2 & \frac{3}{2} & 2 \\ 2 & 2 & 2 & 2 & 1 \end{pmatrix}, \quad \mathcal{A}^{(6)} = \begin{pmatrix} \frac{3}{2} & 2 & 2 & 2 & 1 & 2 \\ 2 & \frac{3}{2} & 2 & 1 & 2 & 2 \\ 2 & 2 & 1 & 2 & 2 & 2 \\ 2 & 1 & 2 & \frac{3}{2} & 2 & 2 \\ 1 & 2 & 2 & 2 & \frac{3}{2} & 2 \\ 2 & 2 & 2 & 2 & 2 & 1 \end{pmatrix}. \quad (4.5)$$

392 The equilibrium points of the system Eq. (4.2) can be obtained by setting the left hand side to be 0, i.e.,

$$X_k(\tilde{\tau}_k - \sum_{j=1}^N a_{k,j} X_j) = 0, \quad X_k \geq 0, \quad \text{for } k = 1, \dots, N. \quad (4.6)$$

393 We denote S as a subset of the set $S_N = \{1, \dots, N\}$ with m entries and \bar{S} to be the complement set of S . The
 394 equilibrium points satisfy $\mathbf{X}_S = 0$ and $\mathcal{A}_{\bar{S}}^{(N)} \mathbf{X}_{\bar{S}} = \tilde{\tau}_{\bar{S}}$, where $\mathcal{A}_{\bar{S}}^{(N)}$ is the square submatrix obtained by removing
 395 all the columns and rows with index in the set S from $\mathcal{A}^{(N)}$. For instance, when $S = \{1, 4\}$, the submatrix $\mathcal{A}_{\bar{S}}^{(N)}$
 396 is defined as a new matrix obtained by removing the first and fourth columns and the first and fourth rows from
 397 $\mathcal{A}^{(N)}$,

$$\mathcal{A}_{\bar{S}}^{(5)} = \begin{pmatrix} \frac{3}{2} & 1 & 2 \\ 1 & \frac{3}{2} & 2 \\ 2 & 2 & 1 \end{pmatrix}, \quad \mathcal{A}_{\bar{S}}^{(6)} = \begin{pmatrix} \frac{3}{2} & 2 & 2 & 2 \\ 2 & 1 & 2 & 2 \\ 2 & 2 & \frac{3}{2} & 2 \\ 2 & 2 & 2 & 1 \end{pmatrix}. \quad (4.7)$$

398 If $\mathcal{A}_{\bar{S}}^{(N)}$ is invertible for all S with $m = 1, \dots, N$, we can at most find 2^N non-negative solutions to Eq. (4.6).

399 **Remark 6.** For a given S , we show that $\mathcal{A}_{\bar{S}}$ is invertible in Appendix A. Thus there exists a solution to the
 400 system $\mathcal{A}_{\bar{S}}^{(N)} \mathbf{X}_{\bar{S}} = \tilde{\tau}_{\bar{S}}$. However, the solution may be negative unless we impose suitable conditions on $\tilde{\tau}_{\bar{S}}$.

401 For succinctness, we will represent $\mathcal{A}^{(N)}$ by \mathcal{A} in the remainder of this section. Linearizing the ODE system
 402 Eq. (4.2) around a equilibrium point $\mathbf{X} = [X_1, X_2, \dots, X_N]^T$ leads to the following eigenvalue problem:

$$\lambda \phi_k = 2 \left(\tilde{\tau}_k - \sum_{j=1}^N a_{k,j} X_j \right) \phi_k - 2X_k \sum_{j=1}^N a_{k,j} \phi_j, \quad 1 \leq k \leq N. \quad (4.8)$$

403 For the equilibrium point satisfying $\mathbf{X}_S = 0$ and $\mathbf{X}_{\bar{S}} = \mathcal{A}_{\bar{S}}^{-1} \tilde{\tau}_{\bar{S}} > 0$, the eigenvalue problem can be decomposed
 404 into two sets of equations:

$$\lambda \phi_k = -2X_k \sum_{j \in \bar{S}} a_{k,j} \phi_j, \quad k \in \bar{S}, \quad (4.9a)$$

405

$$\lambda \phi_k = 2 \left(\tilde{\tau}_k - \sum_{j \in \bar{S}} a_{k,j} X_j \right) \phi_k, \quad k \in S. \quad (4.9b)$$

406 After relabeling, we write Eq. (4.9) in a matrix form

$$\lambda \phi = 2 \begin{pmatrix} -\mathcal{D}_{X_{\bar{S}}} \mathcal{A}_{\bar{S}} & O_{N-m,m} \\ O_{m,N-m} & D_{\tilde{\tau}} \end{pmatrix} \phi, \quad (4.10)$$

407 where $\mathcal{D}_{X_{\bar{S}}}$ is a diagonal matrix with $\mathbf{X}_{\bar{S}}$ on its diagonal, $O_{*,*}$ is a zero matrix and $D_{\tilde{\tau}} = \text{diag}(\mathbf{d}_{\tilde{\tau}})$ is a $m \times m$
 408 diagonal matrix with $\mathbf{d}_{\tilde{\tau}} = [\tilde{\tau}_m - \sum_{j \in \bar{S}} a_{m,j} X_j]$ for $m \in S$. Thus, an eigenvalue of $-\mathcal{D}_{X_{\bar{S}}} \mathcal{A}_{\bar{S}}$ is also an eigenvalue
 409 of Eq. (4.8). We will use this fact to rule out a large part of the unstable equilibrium points. A key observation
 410 is the following lemma.

411 **Lemma 4.** For the equilibrium point satisfying $\mathbf{X}_S = 0$ and $\mathbf{X}_{\bar{S}} = \mathcal{A}_{\bar{S}}^{-1} \tilde{\tau}_{\bar{S}}$, if the matrix $\mathcal{A}_{\bar{S}}$ has a negative
 412 eigenvalue, then the equilibrium point is unstable.

413 *Proof.* It suffices to show that the matrix $-\mathcal{D}_{X_{\bar{S}}} \mathcal{A}_{\bar{S}}$ has a positive eigenvalue when $\mathcal{A}_{\bar{S}}$ has a negative eigenvalue.
 414 A direct computation yields $\mathcal{D}_{X_{\bar{S}}} \mathcal{A}_{\bar{S}}$ is similar to the matrix $\mathcal{D}_{X_{\bar{S}}}^{\frac{1}{2}} \mathcal{A}_{\bar{S}} \mathcal{D}_{X_{\bar{S}}}^{\frac{1}{2}}$, which is congruent to the matrix
 415 $\mathcal{A}_{\bar{S}}$. By Sylvester's law of inertia, the matrix $\mathcal{D}_{X_{\bar{S}}}^{\frac{1}{2}} \mathcal{A}_{\bar{S}} \mathcal{D}_{X_{\bar{S}}}^{\frac{1}{2}}$ and the matrix $\mathcal{A}_{\bar{S}}$ have the same number of positive,
 416 negative and zero eigenvalues. Thus, if $\mathcal{A}_{\bar{S}}$ has a negative eigenvalue, then $-\mathcal{D}_{X_{\bar{S}}} \mathcal{A}_{\bar{S}}$ has a positive eigenvalue. \square

417 Denote $\#S$ as the cardinality of the set S . Regarding the eigenvalues of $\mathcal{A}_{\bar{S}}$, we have the following results:

418 **Lemma 5.** When $\#\bar{S} > 2$, the matrix $\mathcal{A}_{\bar{S}}$ has at least one negative eigenvalue.

419 *Proof.* To prove $\mathcal{A}_{\bar{S}}$ has at least one negative eigenvalue, it suffices to show that $\mathcal{A}_{\bar{S}}$ is not positive semi-definite.
 420 Let $a_{k,j}$ be the entry of $\mathcal{A}_{\bar{S}}$. When $\#\bar{S} > 2$, there exists an index k such that $a_{k+1,k} = a_{k,k+1} = 2$. We choose
 421 $x = [0, \dots, \overbrace{1}^k, -1, \dots, 0]^T$, then $x^T \mathcal{A}_{\bar{S}} x = a_{k,k} - a_{k+1,k} - a_{k,k+1} + a_{k+1,k+1}$. As the entries $a_{k,k}$ and $a_{k+1,k+1}$
 422 are either $\frac{3}{2}$ or 1, we have $x^T \mathcal{A}_{\bar{S}} x = -1, -2$, or $-\frac{3}{2}$. By Sylvester's criterion, $\mathcal{A}_{\bar{S}}$ is not positive semi-definite.
 423 Thus, $\mathcal{A}_{\bar{S}}$ has at least one negative eigenvalue. \square

424 **Lemma 6.** When $\#\bar{S} = 2$, except the matrix

$$\mathcal{A}_{\bar{S}} = \begin{pmatrix} \frac{3}{2} & 1 \\ 1 & \frac{3}{2} \end{pmatrix}, \quad (4.11)$$

425 the matrix $\mathcal{A}_{\bar{S}}$ has at least one negative eigenvalue.

426 *Proof.* When $\#\bar{S} = 2$, the matrix $A_{\bar{S}}$ has the following possible forms:

$$427 \quad \mathcal{A}_{\bar{S}} = \begin{pmatrix} \frac{3}{2} & 1 \\ 1 & \frac{3}{2} \end{pmatrix}, \quad \begin{pmatrix} \frac{3}{2} & 2 \\ 2 & \frac{3}{2} \end{pmatrix}, \quad \text{or} \quad \begin{pmatrix} \frac{3}{2} & 2 \\ 2 & 1 \end{pmatrix}, \quad \text{for } N \text{ is odd,} \quad (4.12)$$

$$428 \quad \mathcal{A}_{\bar{S}} = \begin{pmatrix} \frac{3}{2} & 1 \\ 1 & \frac{3}{2} \end{pmatrix}, \quad \begin{pmatrix} \frac{3}{2} & 2 \\ 2 & \frac{3}{2} \end{pmatrix}, \quad \begin{pmatrix} \frac{3}{2} & 2 \\ 2 & 1 \end{pmatrix}, \quad \text{or} \quad \begin{pmatrix} 1 & 2 \\ 2 & 1 \end{pmatrix} \quad \text{for } N \text{ is even.} \quad (4.13)$$

427 We can easily calculate their eigenvalues explicitly and find that only the eigenvalues of $\mathcal{A}_{\bar{S}} = \begin{pmatrix} \frac{3}{2} & 1 \\ 1 & \frac{3}{2} \end{pmatrix}$ are all
428 positive. \square

429 The above two lemmas have identified most of the unstable equilibrium points. Next, we examine the stability
430 of the remaining equilibrium points.

431 **Lemma 7.** For $\#\bar{S} = 1$ and $\tilde{\tau}_N > \frac{2}{3}\tilde{\tau}_1$,

- 432 • when N is odd, only the equilibrium point $\mathbf{X} = [0, \dots, 0, \tilde{\tau}_N]^\top$ is stable;
- 433 • when N is even, only the equilibrium points $\mathbf{X} = [0, \dots, \tilde{\tau}_{N/2}, \dots, 0]^\top$ and $\mathbf{X} = [0, \dots, 0, \tilde{\tau}_N]^\top$ are stable.

434 *Proof.* For the equilibrium point $\mathbf{X} = [0, \dots, \frac{\tilde{\tau}_k}{a_{k,k}}, \dots, 0]^\top$, the eigenvalue problem Eq. (4.8) can be written in
435 the following matrix form

$$436 \quad \lambda\phi = 2\mathcal{D}_{\tilde{\tau}}\phi, \quad (4.14)$$

436 where $\mathcal{D}_{\tilde{\tau}} = \text{diag}(\mathbf{d})$ is a diagonal matrix with $\mathbf{d} = [\tilde{\tau}_1 - \frac{a_{1,k}}{a_{k,k}}\tilde{\tau}_k, \tilde{\tau}_2 - \frac{a_{2,k}}{a_{k,k}}\tilde{\tau}_k, \dots, -\tilde{\tau}_k, \tilde{\tau}_{k+1} - \frac{a_{k+1,k}}{a_{k,k}}\tilde{\tau}_k, \dots, \tilde{\tau}_N -$
437 $\frac{a_{N,k}}{a_{k,k}}\tilde{\tau}_k]$. Hence, the equilibrium point is unstable if one entry in \mathbf{d} is positive.

- 438 • When N is odd, the $(N - k)$ -th entry of \mathbf{d} is

$$439 \quad \tilde{\tau}_{N-k} - \frac{a_{N-k,k}}{a_{k,k}}\tilde{\tau}_k = \tilde{\tau}_{N-k} - \frac{2}{3}\tilde{\tau}_k > \tilde{\tau}_N - \frac{2}{3}\tilde{\tau}_1 > 0, \quad \text{for } k \neq N. \quad (4.15)$$

439 Thus, the equilibrium point $\mathbf{X} = [0, \dots, \frac{\tilde{\tau}_k}{a_{k,k}}, \dots, 0]^\top$ is unstable for $k \neq N$. Whereas for $k = N$, we have
440 $\lambda_{\max} = 2(\tilde{\tau}_1 - 2\tilde{\tau}_N) < 0$. Therefore, only the equilibrium point $\mathbf{X} = [0, \dots, 0, \tilde{\tau}_N]^\top$ is stable.

- 441 • When N is even, with a similar analysis as done for the odd case, we can show that only the equilibrium
442 points $\mathbf{X} = [0, \dots, \tilde{\tau}_{N/2}, \dots, 0]^\top$ and $\mathbf{X} = [0, \dots, 0, \tilde{\tau}_N]^\top$ are stable.

443 \square

444 **Lemma 8.** For $\#\bar{S} = 2$ and $\tilde{\tau}_N > \frac{2}{3}\tilde{\tau}_1$,

- 445 • when N is odd, the stable equilibrium points are $[0, \dots, X_k, 0, \dots, X_{N-k}, \dots, 0]^\top$ for $k = 1, \dots, \frac{N-1}{2}$, where
446 X_k and X_{N-k} satisfy:

$$447 \quad \begin{pmatrix} \frac{3}{2} & 1 \\ 1 & \frac{3}{2} \end{pmatrix} \begin{pmatrix} X_k \\ X_{N-k} \end{pmatrix} = \begin{pmatrix} \tilde{\tau}_k \\ \tilde{\tau}_{N-k} \end{pmatrix}; \quad (4.16)$$

- 447 • when N is even, the stable equilibrium points are $[0, \dots, X_k, 0, \dots, X_{N-k}, \dots, 0]^\top$ for $k = 1, \dots, \frac{N}{2} - 1$,
448 where X_k and X_{N-k} satisfy:

$$449 \quad \begin{pmatrix} \frac{3}{2} & 1 \\ 1 & \frac{3}{2} \end{pmatrix} \begin{pmatrix} X_k \\ X_{N-k} \end{pmatrix} = \begin{pmatrix} \tilde{\tau}_k \\ \tilde{\tau}_{N-k} \end{pmatrix}. \quad (4.17)$$

449 *Proof.* For compactness, we only prove the case when N is odd. Solving Eq. (4.16) yields

$$450 \quad [X_k, X_{N-k}] = \left[\frac{6}{5}\tilde{\tau}_k - \frac{4}{5}\tilde{\tau}_{N-k}, -\frac{4}{5}\tilde{\tau}_k + \frac{6}{5}\tilde{\tau}_{N-k} \right], \quad (4.18)$$

450 which is positive under the condition that $\tilde{\tau}_N > \frac{2}{3}\tilde{\tau}_1$. The eigenvalue problem Eq. (4.10) becomes

$$451 \quad \lambda\phi = 2 \begin{pmatrix} B & O \\ O & D_{\tilde{\tau}} \end{pmatrix} \phi, \quad (4.19)$$

451 where $D_{\tilde{\tau}} = \text{diag}(\mathbf{d}_{\tilde{\tau}})$ is a $(N - 2) \times (N - 2)$ diagonal matrix with $\mathbf{d}_{\tilde{\tau}} = [\tilde{\tau}_m - a_{m,k}X_k - a_{m,N-k}X_{N-k}]$ for
452 $m \neq k, N - k$ and B is a 2×2 matrix defined by

$$453 \quad B = - \begin{pmatrix} X_k & 0 \\ 0 & X_{N-k} \end{pmatrix} \begin{pmatrix} \frac{3}{2} & 1 \\ 1 & \frac{3}{2} \end{pmatrix}. \quad (4.20)$$

453 The eigenvalue of B is negative, thus we only need to examine the entry of $\mathbf{d}_{\tilde{\tau}}$. When $\tilde{\tau}_N > \frac{2}{3}\tilde{\tau}_1$, we have

$$\tilde{\tau}_m - a_{m,k}X_k - a_{m,N-k}X_{N-k} = \tilde{\tau}_m - \frac{4}{5}(\tilde{\tau}_k + \tilde{\tau}_{N-k}) < \tilde{\tau}_1 - \frac{8}{5}\tilde{\tau}_N < -\frac{1}{10}\tilde{\tau}_N < 0. \quad (4.21)$$

454 Therefore, the equilibrium points $[0, \dots, X_k, 0, \dots, X_{N-k}, \dots, 0]$ for $k = 1, \dots, \frac{N-1}{2}$ are stable. \square

455 We summarize all the above lemmas and obtain our main results.

456 **Proposition 1.** *When $\tilde{\tau}_N > \frac{2\tilde{\tau}_1}{3}$, the system Eq. (4.2) possesses $\lfloor N/2 \rfloor + 1$ stable equilibrium points.*

457 Proposition 1 implies that we can observe at most $\lfloor N/2 \rfloor + 1$ stable oscillatory patterns when $\tilde{\tau}$ is above a
458 certain value.

459 **Remark 7.** *When $\hat{\tau}$ is big enough, the stability of the oscillatory patterns is determined by the direction vectors
460 $\{\mathbf{q}_1, \mathbf{q}_2, \dots, \mathbf{q}_N\}$ that are independent of the spike profile. As the direction vectors are the same for these three
461 singular-perturbed systems, Proposition 1 is valid for all of them.*

462 5 Discussion

463 Temporal oscillations in the pattern position are widely reported in three-component systems [29,30]. For a two-
464 component system that admits stable stationary localized patterns, a simple way of producing traveling patterns
465 is to add a non-diffusive inhabitant to the activator of the two-components systems and increase the reaction-ratio
466 of that inhabitant [26]. In [27], by introducing a second inhibitor to the Schnakenberg model, the coexistence of
467 multiple oscillating patterns is reported and analyzed. However, the number of stable periodic oscillations for an
468 N -spike solution is still unknown. In this article, we extended the analysis to extensions of two other well-known
469 systems the Gierer-Meinhardt system and the Gray-Scot system. Moreover, we rigorously prove, based on the
470 long-time evolution of the amplitudes of the oscillations, that there are at most $\lfloor N/2 \rfloor + 1$ stable patterns for
471 three-component extensions of these systems, thereby resolving the open problem. Our findings shed light on the
472 initiation of rich dynamical behaviors of localized structures. It is worthwhile to note that our analysis is only
473 valid for the bifurcation parameter at an $\mathcal{O}(\varepsilon^2)$ distance to the thresholds. More complex oscillatory patterns,
474 such as zigzag oscillation, when τ exceeds τ_c in an $\mathcal{O}(\varepsilon)$ or $\mathcal{O}(1)$ scale are beyond the scope of this article and
475 need alternative treatments.

476 The new phenomena we observe are not limited to the systems we have studied. In a more realistic situation
477 with more complicated reaction terms and additional diffusion of component w , e.g.

$$\begin{cases} u_t = \varepsilon^2 u_{xx} + f(u, v) - \kappa u w, \\ \tau_v v_t = D_v v_{xx} + g(u, v), \\ \tau_w w_t = D_w \varepsilon^2 w_{xx} + \kappa u w - c w, \\ \text{Neumann boundary conditions at } x = \pm 1. \end{cases} \quad x \in (-1, 1), \quad t \geq 0. \quad (5.1)$$

478 we also observe multiple stable oscillatory moving spikes with suitable parameters. Although the localized profiles
479 of u and w now are unknown analytically, a similar analysis can be done since the localized components, u and
480 w , do not change the stability analysis of the oscillations.

481 Our result is applicable to the system with a uniform feed rate or precursor. It would be interesting to
482 investigate how the heterogeneity impacts the stability threshold as well as the spike dynamics at the onset,
483 which are more biologically relevant because they model the hierarchical formation of small-scale structures
484 induced by large-scale inhomogeneity. Many results exist for two-component systems with heterogeneity. For
485 example, the existence of a solution consisting of a cluster of N spikes near a non-degenerate local minimum
486 point of the smooth inhomogeneity in GM model has been rigorously shown in 1-D [31] and 2-D [32] domains.
487 One future direction is to explore the stability of these spike clusters in three-component systems.

488 For the extended Gierer-Meinhardt system (3.1) with periodic boundary condition, numerical simulations
489 exhibit a traveling and breathing two-spike pattern, which is similar to the moving and breathing solitons
490 discussed in [33]. It is unclear whether such behaviors are due to the same mechanism, i.e., the excitation of both
491 drift and Hopf modes.

492 More complex dynamics are expected in 2-D domains, the freedom in different directions and impact of
493 the domain geometry on the instability remain to be investigated. For example, [24] and [34] employ a hybrid
494 asymptotic-numerical method to investigate the Hopf bifurcation related to translational instabilities for the
495 Schnakenberg model with the high feed rate in two-dimensional domains. Various domains and spot arrangements
496 are numerically tested there, exhibiting rich dynamics. It is an open question to explore these effects on the
497 dynamics of multiple spikes in our extended three-component systems.

498 Appendix A Calculations of \mathcal{A} and $\mathcal{A}_{\bar{5}}$

499 We prove Lemma 3

500 *Proof.* First, we calculate all entries of the matrix \mathcal{A} .

501 Now we calculate the entries on the diagonal of the matrix \mathcal{A} , it is easy to find $a_{N,N} = 1$. When $N = 2n + 1$,
502 for $j = 1, \dots, N - 1$, we have

$$a_{j,j} = N \sum_{l=1}^N Q_{l,j}^4 = \frac{4}{N} \sum_{l=1}^N \sin^4 \frac{(2l-1)j\pi}{2N} = \frac{4}{N} \left(\frac{3N}{8} + \frac{\sin(4j\pi)}{16 \sin \frac{2j\pi}{N}} - \frac{\sin(2j\pi)}{4 \sin \frac{j\pi}{N}} \right) = \frac{3}{2}. \quad (\text{A.1})$$

503 When $N = 2n$, $a_{j,j} = \frac{3}{2}$ for $j \neq n$, N . For $j = n$, we have

$$a_{n,n} = N \sum_{l=1}^N Q_{l,n}^4 = \frac{4}{N} \sum_{l=1}^N \sin^4 \frac{(2l-1)\pi}{4} = \frac{4}{N} \left(\frac{3N}{8} + \frac{1}{8} \sum_{l=1}^N \cos(2l-1)\pi \right) = 1. \quad (\text{A.2})$$

504 Here we use the formula

$$\sin^4 x = \frac{3}{8} + \frac{1}{8} \cos(4x) - \frac{1}{2} \cos(2x), \quad \sum_{k=1}^N \cos(2k-1)x = \frac{\sin(2Nx)}{2 \sin x}, \quad x \neq k\pi \ (k \in \mathbf{N}^+). \quad (\text{A.3})$$

505 Next, we calculate the other entries of the matrix \mathcal{A} . For $i \neq j$ ($i = 1, \dots, N - 1$, $j = 1, \dots, N - 1$) and
506 $i + j \neq N$, we have

$$\begin{aligned} a_{i,j} &= \frac{8}{N} \sum_{l=1}^N \sin^2 \frac{(2l-1)i\pi}{2N} \sin^2 \frac{(2l-1)j\pi}{2N} \\ &= \frac{1}{N} \sum_{l=1}^N \left[\left(\cos \frac{(2l-1)(i+j)\pi}{N} + \cos \frac{(2l-1)(j-i)\pi}{N} \right) - 2 \left(\cos \frac{(2l-1)i\pi}{N} + \cos \frac{(2l-1)j\pi}{N} \right) \right] + 2 \\ &= \frac{1}{N} \left(\frac{\sin(2(i+j)\pi)}{2 \sin \frac{(i+j)\pi}{N}} + \frac{\sin(2(j-i)\pi)}{2 \sin \frac{(j-i)\pi}{N}} \right) - \frac{2}{N} \left(\frac{\sin(2i\pi)}{2 \sin \frac{i\pi}{N}} + \frac{\sin(2j\pi)}{2 \sin \frac{j\pi}{N}} \right) + 2 \\ &= 2. \end{aligned} \quad (\text{A.4})$$

507 For $i + j = N$, we have

$$\begin{aligned} a_{i,j} &= \frac{8}{N} \sum_{l=1}^N \sin^2 \frac{(2l-1)i\pi}{2N} \sin^2 \frac{(2l-1)j\pi}{2N} \\ &= \frac{1}{N} \left[\sum_{l=1}^N \left(\cos(2l-1)\pi + \cos \frac{(2l-1)(j-i)\pi}{N} \right) - 2 \left(\cos \frac{(2l-1)i\pi}{N} + \cos \frac{(2l-1)j\pi}{N} \right) \right] + 2 \\ &= \frac{1}{N} \left(-N + \frac{\sin(2(j-i)\pi)}{2 \sin \frac{(j-i)\pi}{N}} \right) - \frac{2}{N} \left(\frac{\sin(2i\pi)}{2 \sin \frac{i\pi}{N}} + \frac{\sin(2j\pi)}{2 \sin \frac{j\pi}{N}} \right) + 2 \\ &= 1. \end{aligned} \quad (\text{A.5})$$

508 For $i = 1, \dots, N - 1$, we have

$$a_{N,i} = a_{i,N} = \frac{4}{N} \sum_{l=1}^N \sin^2 \frac{(2l-1)i\pi}{2N} = 2 - \frac{2}{N} \sum_{l=1}^N \cos \frac{(2l-1)i\pi}{N} = 2 - \frac{2}{N} \frac{\sin(2i\pi)}{2 \sin \frac{i\pi}{N}} = 2. \quad (\text{A.6})$$

509 Finally, we compute the determinant of \mathcal{A} . We first define the matrix $B_{(2n) \times (2n)}$ as

$$B_{(2n) \times (2n)} = \begin{pmatrix} -\frac{1}{2} & 0 & \cdots & 0 & -1 \\ 0 & -\frac{1}{2} & \cdots & -1 & 0 \\ \vdots & \vdots & \ddots & \vdots & \vdots \\ 0 & -1 & \cdots & -\frac{1}{2} & 0 \\ -1 & 0 & \cdots & 0 & -\frac{1}{2} \end{pmatrix}. \quad (\text{A.7})$$

Using some elementary transformations, we obtain

$$\det(\mathcal{A}) \begin{cases} \frac{r_j - r_N, j=1, \dots, N-1}{r_N + \frac{4}{3}r_i, i=1, \dots, N-1} (1 + \frac{8n}{3}) \det(B_{(2n) \times (2n)}) = (1 + \frac{8n}{3}) \times (-\frac{3}{4})^n, & \text{for } N = 2n + 1, \\ \frac{r_j - r_N, j=1, \dots, N-1}{r_N + \frac{4}{3}r_i, i \neq n, N, r_N + 2r_n} - (\frac{1}{3} + \frac{8n}{3}) \det(B_{(2n-2) \times (2n-2)}) = -(\frac{1}{3} + \frac{8n}{3}) \times (-\frac{3}{4})^{n-1}, & \text{for } N = 2n. \end{cases}$$

510

□

Then we show that $\mathcal{A}_{\bar{S}}$ is invertible.

Recall that S is a subset of the set $S_N = \{1, \dots, N\}$ with m elements, and \bar{S} is the complement of S . $\mathcal{A}_{\bar{S}}$ is the square submatrix obtained by removing all the columns and rows with index in the set S . We shall discuss two cases according to the parity of N . In the following we shall only give details for the case where N is even, the odd case is simpler and we will omit the details.

1. When $N = 2n$, according to whether n and $2n$ belong to S , it will be divided into four cases.

(1). If $\#S = m$ and $n, 2n \in S$, by elementary transformation that exchanges any two rows and corresponding two columns, the original matrix $\mathcal{A}_{\bar{S}}$ can be transformed into the following one

$$\begin{pmatrix} C_{s \times s}(a) & E_{t \times s}^\top \\ E_{t \times s} & D_{t \times t} \end{pmatrix}, \quad (\text{A.8})$$

519 where $s = 2n - 2m + 3$, $t = m - 3$, $a = \frac{3}{2}$ and matrices C, D, E are as follows

$$C_{s \times s}(a) = \begin{pmatrix} \frac{3}{2} & 2 & \cdots & 2 & 1 & 2 \\ 2 & \frac{3}{2} & \cdots & 1 & 2 & 2 \\ \vdots & \vdots & \ddots & \vdots & \vdots & \vdots \\ 2 & 1 & \cdots & \frac{3}{2} & 2 & 2 \\ 1 & 2 & \cdots & 2 & \frac{3}{2} & 2 \\ 2 & 2 & \cdots & 2 & 2 & a \end{pmatrix}, \quad D_{t \times t} = \begin{pmatrix} \frac{3}{2} & 2 & \cdots & 2 \\ 2 & \frac{3}{2} & \cdots & 2 \\ \vdots & \vdots & \ddots & \vdots \\ 2 & 2 & \cdots & \frac{3}{2} \end{pmatrix}, \quad E_{t \times s} = \begin{pmatrix} 2 & 2 & \cdots & 2 \\ 2 & 2 & \cdots & 2 \\ \vdots & \vdots & \ddots & \vdots \\ 2 & 2 & \cdots & 2 \end{pmatrix}. \quad (\text{A.9})$$

Let r_j and c_i represent j -th row and i -th column, respectively. Using some elementary transformations, we have

$$\begin{pmatrix} C_{s \times s}(a) & E_{t \times s}^\top \\ E_{t \times s} & D_{t \times t} \end{pmatrix} \frac{\begin{matrix} r_{2n-2m+3+j} - r_{2n-2m+3}, j=1, \dots, m-3 \\ c_{2n-2m+3+j} - c_{2n-2m+3}, j=1, \dots, m-3 \end{matrix}}{\begin{matrix} r_{2n-2m+3} + \frac{1}{m-2} r_{2n-2m+3+j}, j=1, \dots, m-3 \\ c_{2n-2m+3} + \frac{1}{m-2} c_{2n-2m+3+j}, j=1, \dots, m-3 \end{matrix}} \begin{pmatrix} C_{s_1 \times s_1}(a_1) & O_{t_1 \times s_1}^\top \\ O_{t_1 \times s_1} & F_{t_1 \times t_1} \end{pmatrix}.$$

520 where $s_1 = 2n - 2m + 3$, $t_1 = m - 3$, $a_1 = 2 - \frac{1}{2(m-2)}$, $O_{t_1 \times s_1}$ is a zero matrix and matrix F is as follows

$$F_{t_1 \times t_1} = \begin{pmatrix} -1 & -\frac{1}{2} & \cdots & -\frac{1}{2} \\ -\frac{1}{2} & -1 & \cdots & -\frac{1}{2} \\ \vdots & \vdots & \ddots & \vdots \\ -\frac{1}{2} & -\frac{1}{2} & \cdots & -1 \end{pmatrix}. \quad (\text{A.10})$$

521 Here $r_i - r_j$ means -1 times the j -th row of the matrix is added to the i -th row of the matrix, $c_k - c_l$ means
522 -1 times the l -th column of matrix is added to the i -th column of the matrix. Using the similar method to
523 calculating the determinant of \mathcal{A} , we have

$$\det(C_{s \times s}) = \begin{cases} (\frac{8s-8}{3} + a \frac{-4s+7}{3}) \times (-\frac{3}{4})^{\frac{s-1}{2}}, & \text{for } s \text{ is odd,} \\ -(\frac{8s-4}{3} + a \frac{-4s+5}{3}) \times (-\frac{3}{4})^{\frac{s-2}{2}}, & \text{for } s \text{ is even.} \end{cases} \quad (\text{A.11})$$

524 and

$$\det(F_{t \times t}) = \frac{r_1 + r_j, j=2, \dots, t}{r_j - \frac{1}{t+1} r_1, j=2, \dots, t} \left(-\frac{1}{2}\right)^t \times (t+1) \quad (\text{A.12})$$

Therefore we have

$$|\det(\mathcal{A}_{\bar{S}})| = \left| \frac{4n}{3} + \frac{2m}{3} - \frac{19}{6} \right| \times \left(\frac{3}{4}\right)^{n-m+1} \times \left(\frac{1}{2}\right)^{m-3}.$$

(2). If $\#S = m$ and $n, 2n \notin S$, by elementary transformation that exchanges any two rows and corresponding two columns, the original matrix $\mathcal{A}_{\bar{S}}$ can be transformed into (A.8), where $s = 2n - 2m$, $t = m$, $a = 1$. Again

using elementary transformations, we have

$$\begin{pmatrix} C_{s \times s}(a) & E_{t \times s}^\top \\ E_{t \times s} & D_{t \times t} \end{pmatrix} \xrightarrow{\begin{array}{l} r_{2n-2m+1+j} - r_{2n-2m+1}, \quad j=1, \dots, m-1 \\ c_{2n-2m+1+j} - c_{2n-2m+1}, \quad j=1, \dots, m-1 \\ r_{2n-2m+1} + \frac{1}{m} r_{2n-2m+1+j}, \quad j=1, \dots, m-1 \\ c_{2n-2m+1} + \frac{1}{m} c_{2n-2m+1+j}, \quad j=1, \dots, m-1 \\ r_{2n-2m+1} - r_{2n-2m}, \quad c_{2n-2m+1} - c_{2n-2m} \\ r_{2n-2m} + \frac{2m}{2m+1} r_{2n-2m+1}, \quad c_{2n-2m} + \frac{2m}{2m+1} c_{2n-2m+1} \end{array}} \begin{pmatrix} C_{s_2 \times s_2}(a_2) & \mathbf{0}_1 & O_{t_2 \times s_2}^\top \\ \mathbf{0}_1^\top & -\frac{2m+1}{2m} & \mathbf{0}_2^\top \\ O_{t_2 \times s_2} & \mathbf{0}_2 & F_{t_2 \times t_2} \end{pmatrix},$$

where $s_2 = 2n - 2m$, $t_2 = m - 1$, $a_2 = 2 - \frac{1}{2m+1}$, $\mathbf{0}_1 = (0, \dots, 0)^\top$ and $\mathbf{0}_2 = (0, \dots, 0)^\top$ are s_2 -dimensional column vector and t_2 -dimensional column vector, respectively. By (A.11) and (A.12), we get

$$|\det(\mathcal{A}_{\bar{S}})| = \left(\frac{4n}{3} + \frac{2m}{3} + \frac{1}{6} \right) \times \left(\frac{3}{4} \right)^{n-m-1} \times \left(\frac{1}{2} \right)^{m-1}.$$

(3). If $\#S = m$ and $2n \in S$, $n \notin S$, by elementary transformation that exchanges any two rows and corresponding two columns, the original matrix $\mathcal{A}_{\bar{S}}$ can be transformed into (A.8), where $s = 2n - 2m + 2$, $t = m - 2$, $a = \frac{3}{2}$. Again using elementary transformations, we have

$$\begin{pmatrix} C_{s \times s}(a) & E_{t \times s}^\top \\ E_{t \times s} & D_{t \times t} \end{pmatrix} \xrightarrow{\begin{array}{l} r_{2n-2m+2+j} - r_{2n-2m+2}, \quad j=1, \dots, m-2 \\ c_{2n-2m+2+j} - c_{2n-2m+2}, \quad j=1, \dots, m-2 \\ r_{2n-2m+2} + \frac{1}{m-1} r_{2n-2m+2+j}, \quad j=1, \dots, m-2 \\ c_{2n-2m+2} + \frac{1}{m-1} c_{2n-2m+2+j}, \quad j=1, \dots, m-2 \end{array}} \begin{pmatrix} C_{s_3 \times s_3}(a_3) & O_{t_3 \times s_3}^\top \\ O_{t_3 \times s_3} & F_{t_3 \times t_3} \end{pmatrix}.$$

where $s_3 = 2n - 2m + 2$, $t_3 = m - 2$, $a_3 = 2 - \frac{1}{2(m-1)}$. By (A.11) and (A.12), we have

$$|\det(\mathcal{A}_{\bar{S}})| = \left| \frac{4n}{3} + \frac{2m}{3} - \frac{3}{2} \right| \times \left(\frac{3}{4} \right)^{n-m} \times \left(\frac{1}{2} \right)^{m-2}.$$

(4). If $\#S = m$ and $n \in S$, $2n \notin S$, by elementary transformation that exchanges any two rows and corresponding two columns, the original matrix $\mathcal{A}_{\bar{S}}$ can be transformed into (A.8), where $s = 2n - 2m + 1$, $t = m - 1$, $a = 1$. Again using elementary transformations, we have

$$\begin{pmatrix} C_{s \times s}(a) & E_{t \times s}^\top \\ E_{t \times s} & D_{t \times t} \end{pmatrix} \xrightarrow{\begin{array}{l} r_{2n-2m+2+j} - r_{2n-2m+2}, \quad j=1, \dots, m-2 \\ c_{2n-2m+2+j} - c_{2n-2m+2}, \quad j=1, \dots, m-2 \\ r_{2n-2m+2} + \frac{1}{m-1} r_{2n-2m+2+j}, \quad j=1, \dots, m-2 \\ c_{2n-2m+2} + \frac{1}{m-1} c_{2n-2m+2+j}, \quad j=1, \dots, m-2 \\ r_{2n-2m+2} - r_{2n-2m+1}, \quad c_{2n-2m+2} - c_{2n-2m+1} \\ r_{2n-2m+1} + \frac{2m-2}{2m-1} r_{2n-2m+2}, \quad c_{2n-2m+1} + \frac{2m-2}{2m-1} c_{2n-2m+2} \end{array}} \begin{pmatrix} C_{s_4 \times s_4}(a_4) & \mathbf{0}_1 & O_{t_4 \times s_4}^\top \\ \mathbf{0}_1^\top & -\frac{2m-1}{2m-2} & \mathbf{0}_2^\top \\ O_{t_4 \times s_4} & \mathbf{0}_2 & F_{t_4 \times t_4} \end{pmatrix},$$

where $s_4 = 2n - 2m + 1$, $t_4 = m - 2$, $a_4 = 2 - \frac{1}{2m-1}$, $\mathbf{0}_1 = (0, \dots, 0)^\top$ and $\mathbf{0}_2 = (0, \dots, 0)^\top$ are s_4 -dimensional column vector and t_4 -dimensional column vector, respectively. By (A.11) and (A.12), we have

$$|\det(\mathcal{A}_{\bar{S}})| = \left| \frac{4n}{3} + \frac{2m}{3} - \frac{3}{2} \right| \times \left(\frac{3}{4} \right)^{n-m} \times \left(\frac{1}{2} \right)^{m-2}.$$

2. When $N = 2n + 1$, by (A.11) and (A.12) we have

$$|\det(\mathcal{A}_{\bar{S}})| = \begin{cases} \left| \frac{4n}{3} + \frac{2m}{3} - \frac{7}{6} \right| \times \left(\frac{3}{4} \right)^{n-m+1} \times \left(\frac{1}{2} \right)^{m-2}, & \text{for } \#S = m \text{ and } 2n + 1 \in S, \\ \left| \frac{4n}{3} + \frac{2m}{3} + \frac{1}{2} \right| \times \left(\frac{3}{4} \right)^{n-m} \times \left(\frac{1}{2} \right)^{m-1}, & \text{for } \#S = m \text{ and } 2n + 1 \notin S. \end{cases}$$

References

525

526

527

528

529

530

531

532

533

534

- [1] V. K. Vanag and I. R. Epstein, "Localized patterns in reaction-diffusion systems," *Chaos: An Interdisciplinary Journal of Nonlinear Science*, vol. 17, no. 3, p. 037110, 2007.
- [2] A. Gierer and H. Meinhardt, "A theory of biological pattern formation," *Kybernetik*, vol. 12, no. 1, pp. 30–39, 1972.
- [3] J. E. Pearson, "Complex patterns in a simple system," *Science*, vol. 261, no. 5118, pp. 189–192, 1993.
- [4] J. Schnakenberg, "Simple chemical reaction systems with limit cycle behaviour," *Journal of theoretical biology*, vol. 81, no. 3, pp. 389–400, 1979.
- [5] A. Doelman, R. A. Gardner, and T. J. Kaper, "Large stable pulse solutions in reaction-diffusion equations," *Indiana University Mathematics Journal*, vol. 50, no. 1, pp. 443–507, 2001.

- 535 [6] A. Doelman, T. J. Kaper, and H. van der Ploeg, “Spatially periodic and aperiodic multi-pulse patterns
536 in the one-dimensional Gierer-Meinhardt equation,” *Methods and applications of analysis*, vol. 8, no. 3,
537 pp. 387–414, 2001.
- 538 [7] D. Iron, M. J. Ward, and J. Wei, “The stability of spike solutions to the one-dimensional Gierer-Meinhardt
539 model,” *Physica D. Nonlinear Phenomena*, vol. 150, no. 1-2, pp. 25–62, 2001.
- 540 [8] D. Iron and M. J. Ward, “The dynamics of multispikes solutions to the one-dimensional Gierer-Meinhardt
541 model,” *SIAM Journal on Applied Mathematics*, vol. 62, no. 6, pp. 1924–1951, 2002.
- 542 [9] D. Gomez, L. Mei, and J. Wei, “Hopf bifurcation from spike solutions for the weak coupling Gierer-Meinhardt
543 system,” *European Journal of Applied Mathematics*, vol. 32, no. 1, pp. 113–145, 2021.
- 544 [10] M. J. Ward and J. Wei, “Hopf bifurcation of spike solutions for the shadow Gierer-Meinhardt model,”
545 *European Journal of Applied Mathematics*, vol. 14, no. 6, pp. 677–711, 2003.
- 546 [11] M. J. Ward and J. Wei, “Hopf bifurcations and oscillatory instabilities of spike solutions for the one-
547 dimensional Gierer-Meinhardt model,” *Journal of Nonlinear Science*, vol. 13, no. 2, pp. 209–264, 2003.
- 548 [12] J. Wei and M. Winter, *Mathematical aspects of pattern formation in biological systems*, vol. 189. Springer
549 Science & Business Media, 2013.
- 550 [13] A. Doelman, R. A. Gardner, and T. J. Kaper, *A stability index analysis of 1-D patterns of the Gray-Scott
551 model*. Memoirs of the American Mathematical Society, 2002.
- 552 [14] A. Doelman, T. J. Kaper, and P. A. Zegeling, “Pattern formation in the one-dimensional Gray-Scott model,”
553 *Nonlinearity*, vol. 10, no. 2, pp. 523–563, 1997.
- 554 [15] T. Kolokolnikov, M. J. Ward, and J. Wei, “The existence and stability of spike equilibria in the one-
555 dimensional Gray-Scott model: The low feed-rate regime,” *Studies in Applied Mathematics*, vol. 115, no. 1,
556 pp. 21–71, 2005.
- 557 [16] T. Kolokolnikov, M. J. Ward, and J. Wei, “The existence and stability of spike equilibria in the one-
558 dimensional Gray-Scott model: The pulse-splitting regime,” *Physica D. Nonlinear Phenomena*, vol. 202,
559 no. 3-4, pp. 258–293, 2005.
- 560 [17] D. Gomez, L. Mei, and J. Wei, “Stable and unstable periodic spiky solutions for the Gray-Scott system and
561 the Schnakenberg system,” *Journal of Dynamics and Differential Equations*, vol. 32, no. 1, pp. 441–481,
562 2020.
- 563 [18] T. Kolokolnikov, M. J. Ward, and J. Wei, “Slow translational instabilities of spike patterns in the one-
564 dimensional Gray-Scott model,” *Interfaces and Free Boundaries*, vol. 8, no. 2, pp. 185–222, 2006.
- 565 [19] D. Iron, J. Wei, and M. Winter, “Stability analysis of Turing patterns generated by the Schnakenberg
566 model,” *Journal of mathematical biology*, vol. 49, no. 4, pp. 358–390, 2004.
- 567 [20] M. J. Ward and J. Wei, “The existence and stability of asymmetric spike patterns for the Schnakenberg
568 model,” *Studies in Applied Mathematics*, vol. 109, no. 3, pp. 229–264, 2002.
- 569 [21] T. Kolokolnikov, F. Paquin-Lefebvre, and M. J. Ward, “Competition instabilities of spike patterns for the
570 1D Gierer-Meinhardt and Schnakenberg models are subcritical,” *Nonlinearity*, vol. 34, no. 1, pp. 273–312,
571 2021.
- 572 [22] F. Veerman, “Breathing pulses in singularly perturbed reaction-diffusion systems,” *Nonlinearity*, vol. 28,
573 no. 7, pp. 2211–2246, 2015.
- 574 [23] W. Chen and M. J. Ward, “Oscillatory instabilities and dynamics of multi-spike patterns for the one-
575 dimensional Gray-Scott model,” *European Journal of Applied Mathematics*, vol. 20, no. 2, pp. 187–214,
576 2009.
- 577 [24] S. Xie and T. Kolokolnikov, “Moving and jumping spot in a two-dimensional reaction-diffusion model,”
578 *Nonlinearity*, vol. 30, no. 4, pp. 1536–1563, 2017.
- 579 [25] W. Chen and M. J. Ward, “The stability and dynamics of localized spot patterns in the two-dimensional
580 Gray-Scott model,” *SIAM Journal on Applied Dynamical Systems*, vol. 10, no. 2, pp. 582–666, 2011.
- 581 [26] M. Or-Guil, M. Bode, C. Schenk, and H.-G. Purwins, “Spot bifurcations in three-component reaction-
582 diffusion systems: The onset of propagation,” *Physical Review E*, vol. 57, no. 6, pp. 6432–6437, 1998.
- 583 [27] S. Xie, T. Kolokolnikov, and Y. Nishiura, “Complex oscillatory motion of multiple spikes in a three-
584 component Schnakenberg system,” *Nonlinearity*, vol. 34, no. 8, pp. 5708–5743, 2021.
- 585 [28] P. S. Inc., “Flexpde 7,” <https://www.pdesolutions.com/index.html>, 2020.
- 586 [29] S. Gurevich, S. Amiranashvili, and H.-G. Purwins, “Breathing dissipative solitons in three-component
587 reaction-diffusion system,” *Physical Review E*, vol. 74, no. 6, p. 066201, 2006.

- 588 [30] V. Giunta, M. C. Lombardo, and M. Sammartino, “Pattern formation and transition to chaos in a chemotaxis
589 model of acute inflammation,” *SIAM Journal on Applied Dynamical Systems*, vol. 20, no. 4, pp. 1844–1881,
590 2021.
- 591 [31] J. Wei and M. Winter, “Stable spike clusters for the one-dimensional Gierer-Meinhardt system,” *European*
592 *Journal of Applied Mathematics*, vol. 28, no. 4, pp. 576–635, 2017.
- 593 [32] J. Wei, M. Winter, and W. Yang, “Stable spike clusters for the precursor Gierer-Meinhardt system in \mathbb{R}^2 ,”
594 *Calculus of Variations and Partial Differential Equations*, vol. 56, no. 5, p. 142, 2017.
- 595 [33] S. Gurevich and R. Friedrich, “Moving and breathing localized structures in reaction-diffusion systems,”
596 *Mathematical Modelling of Natural Phenomena*, vol. 8, no. 5, pp. 84–94, 2013.
- 597 [34] J. Tzou and S. Xie, “Oscillatory translational instabilities of spot patterns in the schnakenberg system on
598 general 2d domains,” *Nonlinearity*, vol. 36, no. 5, p. 2473, 2023.